Master's thesis in Electric Power Engineering

Investigation on the Performance of a Modular Multi-level Converter (MMC) based UPS System

JOHN WALUSIMBI KIGOZI

CHALMERS
UNIVERSITY OF TECHNOLOGY

Department of Energy and Environment
Division of Electric Power Engineering
Chalmers University of Technology
Göteborg, Sweden 2016

Investigation on the Performance a Modular Multilevel Converter (MMC) based UPS Systems.
JOHN WALUSIMBI KIGOZI

Supervisors: Fredrik Lundmark
WSP-Sverige SE-402 51
Electric Power Systems
Gothenburg -Sweden
Email: fredrik.lundmark@wspgroup.se

Mattias Hermansson
WSP-Sverige SE-402 51
Electric Power Systems
Gothenburg -Sweden
Email: mattias.hermansson@wspgroup.se

Examiner : Prof. Massimo Bongiorno
Division of Electric Power Engineering
Department of Energy and Environment
Chalmers University of Technology SE-412 96
Gothenburg-Sweden
Email: massimo.bongiorno@chalmers.se

Division of Electric Power Engineering
Department of Energy and Environment
CHALMERS UNIVERSITY OF TECHNOLOGY
Göteborg, Sweden 2016

Investigation on the Performance a Modular Multilevel Converter (MMC) based UPS Systems
JOHN WALUSIMBI KIGOZI

Division of Electric Power Engineering
Department of Energy and Environment
CHALMERS UNIVERSITY OF TECHNOLOGY
SE-412 96 Göteborg
Sweden
Telephone +46(0)31-7721000

Chalmers Bibliotek, Reproservice
Göteborg, Sweden 2016

Investigation on the performance Modular Multi-level Converters (MMC) based UPS Systems
JOHN WALUSIMBI KIGOZI
Division of Electric Power Engineering
Department of Energy and Environment
Chalmers University of Technology

Abstract

An Uninterruptible Power Supply (UPS) is a custom power device commonly used in Low voltage networks to protect sensitive loads by mitigating power quality problems like voltage dips, interruptions and improvement of power factor. Sudden power outages, that are unplanned and power disturbances in unprotected low and medium voltage networks with sensitive load of a duration ranging from a hundreds of milliseconds to several hours could eventuate into adverse financial losses. In this thesis, a study is performed on the state of the art developments in UPS designs and available topologies commonly used in the industry with static converters. A Modular Multi-level Converter (MMC) based UPS system is proposed and simulated in Matlab/SIMULINK with PLECS blockset under different operating conditions such as load unbalance, voltage dips and operation with both resistive-inductive and non-linear loads with a focus on converter performance. The UPS system is compared the Two-level Voltage Source Converter (VSC) based UPS topology. The results showed that the output voltage wave forms of the Medium Voltage (MV) MMC have a more sinusoidal shape compared with the Two-level converter that has a square output voltage, hence less requirements on the filters for the MMC. In the thesis an MMC UPS was simulated with a switching frequency of 1000Hz which was significantly lower than the 2000Hz for Two-level converter based UPS system, resulting in lower losses when using the MMC based UPS system. The structure and operation of the MMC was described and it showed that series modules could be added in the arms of the MMC to alter its operating voltage and power requirement, offering system scalability. With the structure of MMCs, it's possible to perform cell hot swaps and this increases the reliability of the MMC UPS as modules can be replaced while UPS still remains in operation without necessarily invoking the maintenance by-pass mode. In the MMC, the failed module can also be by-passed, thus offering very high redundancy and possibility to use low cost valves in the modules. The risks of operating the MV MMC and Transformerless UPS systems are also discussed and suggestions are made on how to manage the risks. Finally practical scenarios are identified where the proposed MMC based UPS systems can be applied in industry and how they can improve on the power quality and reduce on the operational losses.

Keywords: Power Quality, Voltage Source Converter(VSC), Custom Power device, Uninterruptible Power Supply(UPS), Modular Multi-level Converter(MMC)

Acknowledgements

This thesis was carried out at the Electric Power Systems department at WSP-Sverige, Göteborg in cooperation with Department of Energy and Environment at Chalmers University.

My studies at Chalmers were made possible through sponsorship from the Swedish Institute. Firstly and foremost, I thank my supervisor and examiner at Chalmers, Prof. Massimo Bongiorno for his patience and advice from the point developing the thesis idea through the entire thesis period and also helping me with PLECS. I also acknowledge other teachers and tutors at Chalmers who have taught me various modules in the electric power discipline.

I extend special thanks to my supervisors at WSP Systems, Fredrik Lundmark and Mattias Hermansson for initiating the thesis opportunity, providing me with technical guidance and logistical support as well. I also like to thank WSP and all its staff for providing a calm and friendly working atmosphere. It worth to mention the likes of Jacob Edvinsson, Helen Jarlros and Martin Skoglund at the Power Systems department of WSP.

Contents

List of Figures

1

Introduction

1.1 Background and motivation

An Uninterruptible Power Supply (UPS) is a custom power device used to mitigate power quality problems in low voltage distribution system. UPSs find many applications in Hospitals, Data Centres, Industrial facilities, military installations, telecom facilities and Emergency Power Systems (EPS) in Nuclear Power Plants (NPP). They are used to protect critical loads that are susceptible to power spikes, voltage dips, supply frequency variations, brown-outs [1] and power interruption ranging from a few milliseconds to several hours [2].

A study presented in [3] on the cost of un-planned power outages in the industrial, retail, public and agricultural sectors in Sweden in 2005 revealed all the aforementioned sectors had experienced outages ranging from a minute to several hours over the past 12 months resulted in damage of products, re-scheduling activities and financial loss through damage claims among other costs. In [3] at least 45% of all these sectors players had no means of protecting themselves from these power disturbances, while only 26% utilized UPS systems and 9% relied on insurance in the industrial sector to safeguard themselves from the consequences of the power disturbances. The level of protection against power disturbances in Sweden using UPS is still low yet some industries continue to pay the price for low power quality and disturbances in Low and Medium Voltage distribution networks.

For those that are using UPS systems, there is a vast increase in the number of UPS topologies on the market ranging from Rotary UPS systems to a number of Static based (Power Electronic) UPS systems with different converter topologies over the years. As these UPS topologies evolve on the market, there is need to fast track and adapt the UPS technologies to existing installations as well as new installations. A basic example could be adapting the grounding system to the new UPS topologies which is responsible for enabling the protection systems to function well and clear ground faults and also protects sensitive load as well as the UPS systems [4] . The grounding system is dependent on the configuration of the UPS and the nature of the connected load [4] . It is therefore necessary to study the topologies from the device level, to the system level and observe how the components are controlled and how they interact together to enhance the power quality and reliability in low voltage power system.

It is with this background that, the performance of UPS systems based on MMCs is compared with traditional Two-level converters for application in Emergency Power Systems(EPS) at Low and Medium voltage distribution networks to establish their benefits and challenges. MMCs can allow for transformerless grid connections, distributed energy storage among the modules, increased reliability, and offer scalability by connecting the modules in series [5]. The Modular Multi-level Converter is shown in Figure 1.1 below where SM is the sub-module $j\,(1 < j < 2N)$ located in phase $x = (a, b, c)$

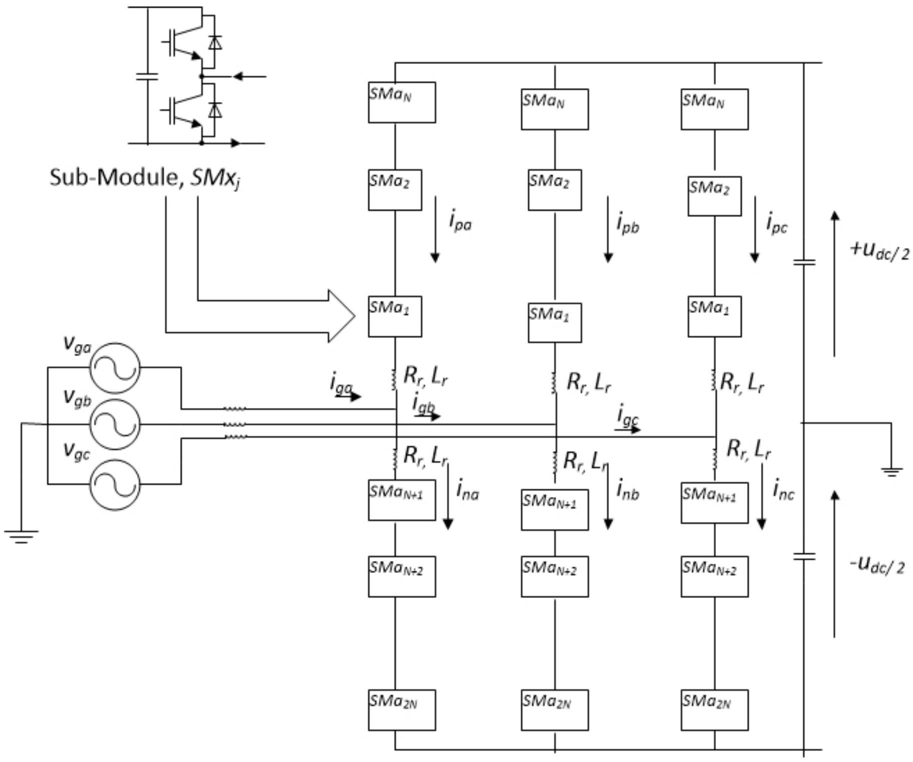

Figure 1.1: Structure of the Modular Multi-level Converter

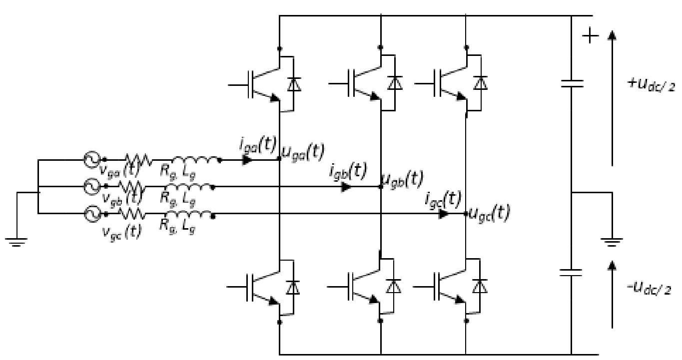

Figure 1.2: Structure of the Two-level Converter

1.2 Current Work

In the past years there has been a lot of research effort on applications of Multi-level Converters for HVDC Transmission systems [4]. However, today there are plenty of applications of the multilevel converters even at Low voltage systems as well, where they have replaced the traditional Two-level converter systems with the major goal of reducing wave distortions from the converter [6].

In [6], the author discussed the possibilities to use Multi-level converters for UPS applications. The converters covered in [6] included the three-level diode-clamped and the four-level diode-clamped Multi-level converters but did not discuss the possibility of using Modular Multi-level Converters. Various applications of MMCs in Medium as well as Low voltage systems with half bridges have also been studied in [5][7].

An investigation on the feasibility of connecting a UPS system at Medium Voltage (20 kV) has been done before in [8] on an existing distribution network and it showed a significant improvement in power quality. In [8], the authors considered a Rotary UPS system with a Flywheel. However, with the advent and development of MMC in HVDC it is also possible to have a VSC at higher voltages levels that can be utilized in the MV Static UPS systems for Power quality improvement and loss reduction for high power applications in LV distribution system.

1.3 Aims

The purpose of this study is perform a study on UPS topologies in the industry and to evaluate the performance of the proposed UPS system with Modular Multi-level Converters in comparison to the traditional Two-level based UPS systems. A Modular Multi-level Converter based UPS is implemented in Matlab/SIMULINK with PLECS Blockset. A case study is selected to demonstrate where the UPS system can be applied in practice and its performance is studied.

2

Uninterruptible Power Supply Topologies

2.1 Rotary UPS Systems

This type of UPS topology utilizes the motor-generator set and it is a classical way of mitigating voltage dips [9] and interruptions for a few seconds. Rotary systems find applications where the power requirements are somewhat high, typically 125kVA and above [10]. These systems consist of three basic building blocks, that is: the motor, generator and a flywheel, see Figure 2.1. The motor-generator set offers high efficiency, fault handling capability and tolerance when used to supply loads with high inrush currents [10] in noisy environments. However this kind of topology is expensive when it comes to maintenance, since it consists of mechanical moving parts thus it is prone to wear and tear making it to require periodic maintenance. This topology is also characterised by high noise production and high system losses due to friction in the mechanical moving parts [9] [10].

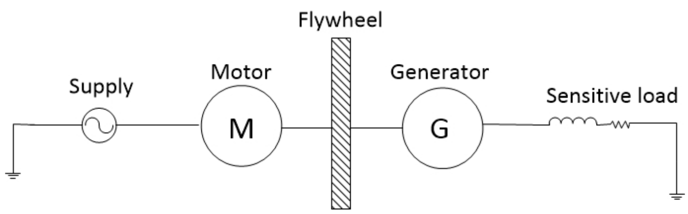

Figure 2.1: Rotary UPS System

Principles of rotary UPS systems

The motor is mechanically coupled to the flywheel and the synchronous generator at the supply frequency. During normal operation, the voltage regulator regulates the generator voltage and the system frequency is maintained. When there is a short interruption or voltage dips, then the flywheel will transfer its stored to the generator to maintain its frequency within the pre-determined limits for a time duration that is determined by the inertia of the flywheel [10]. The autonomy time of the UPS system is very short compared to that of the Static UPSs and these UPS systems can only be used to bridge short disturbances or until the diesel generators are started to provide backup.

2.2 Static UPS System

The Swedish Standard, SS-EN 62040-1 for general and safety requirements for UPS defines a UPS as “a combination of converters, switches and energy storage devices that make up a power system for maintaining continuity of the load power in case of failure of the input-power” , as well as improving the power quality of the electric supply. The SS-EN 62040-1 has no provisions for Rotary UPS systems. In this thesis from here and thereafter when the word “UPS” is used, reference will be made to a Static UPS system unless specificity to a Rotary UPS is stated. A static UPS system is constituted by a rectifier, an Inverter and an energy storage mounted in the DC link [10] as shown in Figure 2.2. The structure of the Static UPS can closely be related to that of the variable speed drive with the only difference being that the UPS has an energy storage connected to the DC bus [9]. Static UPS systems come in three main topologies, namely; Single-conversion Static UPS systems, Double-conversion Static systems and Multi-mode Static UPS systems.

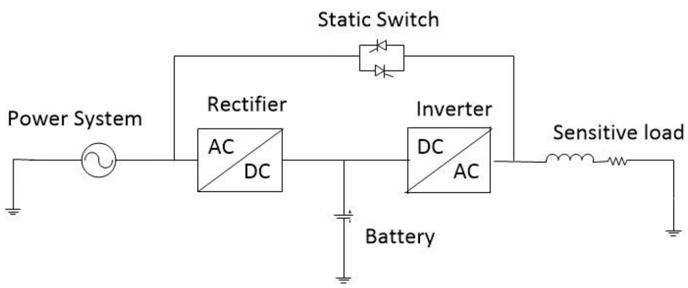

Figure 2.2: Static UPS System

2.2.1 Single-conversion Static UPS systems

This UPS operates on the batteries in the event of a disturbance from the grid supply such as an interruption or a power quality phenomenon for example a voltage dip. The topology transfers sensitive load back to the mains with the help of static transfer switches under normal operation. The direction of power flow in this topology is shown in the Figure 2.3 [11].

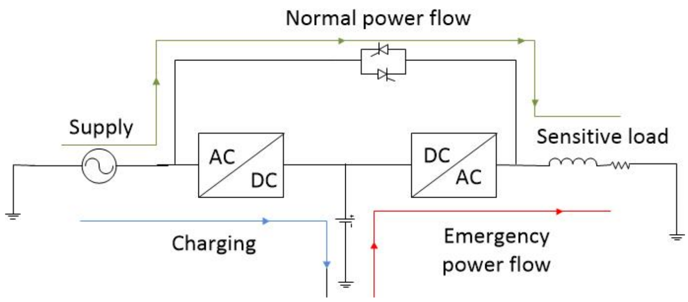

Figure 2.3: Single conversion UPS System

2.2.2 Double-conversion Static UPS systems

In the double conversion topology, like its name suggests, it has two power conversion stages from AC mains to DC to charge the battery pack and finally to AC at the load connection point [11]. It protects the load by isolating it from a direct connection to the grid supply side. The direction of power flow for double conversion UPS topology is shown in the Figure 2.4. This is of a lower cost compared to the multi-mode topology but has very lower efficiency because of the double power conversion process.

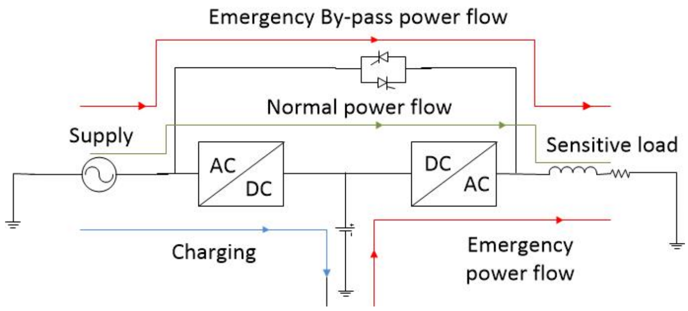

Figure 2.4: Double Conversion UPS System

2.2.3 Multi-mode Static UPS systems

This static UPS system combines the good features of the double as well as the single conversion UPS system thus achieving improved reliability and efficiency [11]. During normal operation, the UPS system operates in Mode 1 (see Figure 2.5). In the event of occurrence of a disturbance from the supply side it automatically transfers the sensitive load to Mode 2, which is the double conversion in a bid to ensure maximum protection of the load but compromising system efficiency. If the power quality of the supply drops below preset tolerances for the rectifier during the operation under mode 2, the load will then be finally transferred to the battery packs [11]. Restoration of the mains supply takes the operation back to Mode 1 of operation. This topology is very energy efficient but more costly than its counterparts.The conversion between different modes of the topology is governed by the characteristics of the static transfer switches.

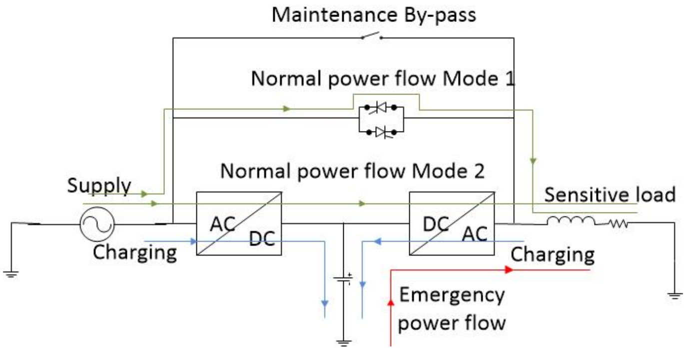

Figure 2.5: Modular Multi-mode UPS System

2.3 Transformer based and Transformerless UPS Systems

2.3.1 Transformer based UPS systems

The transformer based UPS system consists of a battery pack directly connected to the DC link. The UPS converter on the grid side consists of either a 6-pulse or 12-pulse Silicon Controlled Rectifier (SCR) rectifiers at its input and an isolation transformer to provide galvanic isolation of the AC side from the DC link and passive fault management by adding impedance in the circuit as shown in the Figure 2.6a and 2.6b[12]. The isolation transformer at the output of the UPS provides a local solid neutral-ground which enables common mode noise rejection [12].

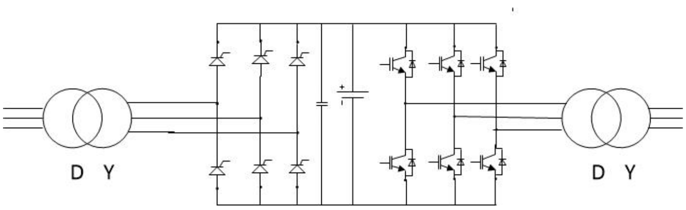

(a)

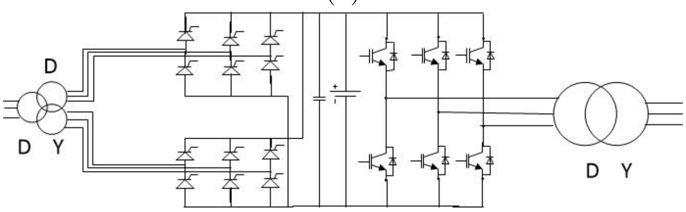

(b)

Figure 2.6: Transformer Based UPS Systems (a) 6-Pulse and (b) 12-Pulse.

A natural operating characteristic of a six-pulse rectifier is the generation of harmonic currents on the input source. A six-pulse rectifier will generate a total harmonic current distortion (THD) of greater than 30 percent [13]. Because of this reason, the transformer based topology is in two common configurations namely; 6-pulse configurations in Figure 2.6a above and 12-pulse configuration in Figure 2.6b to provide filtering to meet the set standards for maximum harmonic pollution.

2.3.2 Transformerless UPS systems

In transformerless UPS systems, the DC-DC converter enables the battery pack to be connected to the DC link of the UPS. In the transformerless UPS system only IGBTs are used for all the power conversion stages [14]. There is no direct connection of the batteries to the DC link as shown in Figure 2.7. In this topology IGBTs they have faster switching speeds than thyristors and can easily be controlled by on and off signals applied to the gate terminal of the device unlike for thyristors where you have to wait for the zero crossing [14].

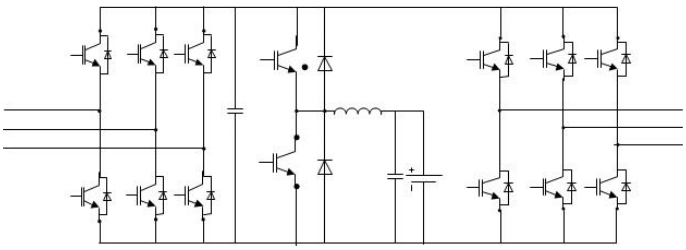

Figure 2.7: Transformerless UPS System

In this topology, it is necessary to phase out the chance of a DC fault from propagating to the AC side by equipping the UPS with active fault management strategies. This topology has a higher efficiency since it uses power electronics unlike passive components. It has a relatively lower price and requires a smaller footprint area.

3

Voltage Source Converters for UPS Applications

3.1 Power Semi-conductors for UPS applications

The basic building blocks for Static UPS Converters are power semiconductors and these include: Diodes, MOSFETS, Thyristors, GTOs, BJTs and IGBTS. The choice of selection of the device to be used depends upon the power as well as the voltage level for the UPS application.

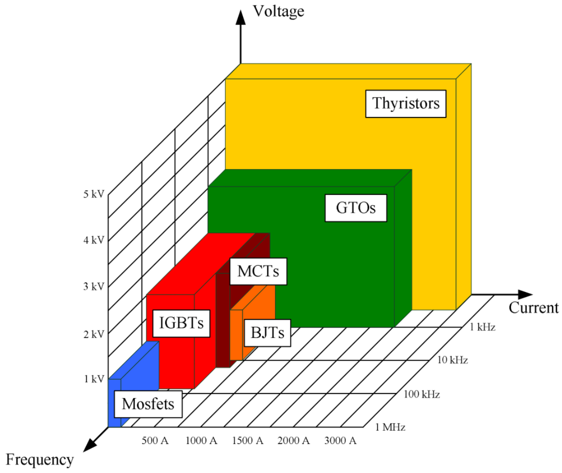

Figure 3.1: Performance evaluation of Power electronic semi-conductors

Figure 3.1 [15] shows the comparison of power semiconductors for various applications in-terms of power handling capabilities as well as switching speeds. Since the UPS is a custom power device at Low voltage and Medium voltage, then it is necessary for the choice of power semi-conductor to have capability to respond fast to disturbance owing to poor power quality, while also being able to handle the power and voltage level in the application in which the UPS is to be used. For UPS applications at Low and Medium Voltage, IGBTs and Thyristors are commonly used to design the converters owing to their relatively faster switching speeds and their ability to handle the low voltage as well as the Medium voltage.

Thyristors

These devices can be fired on if a positive pulse is applied to its gate terminal for a very short duration when it is forward biased [16]. The Thyristor can be used at high voltages up-to 6000V and current of thousands of Amps with a low forward voltage drop [17]. Because of its reliability and relatively lower cost [17], it finds application in the state of art large UPS systems in the rectifier stage in the kVA range both in the six pulse and twelve pulse configuration converter system. It can also applied in designing static transfer switches

IGBT

These devices combine the good properties of the BJT, MOSFETs and GTOs [16]. With fast switching time of about 300 ns for power levels like those of the BJT with improved voltage control despite a large forward voltage drop of about 3 V for 1200V [17]. IGBTs are used in the state of the art PWM transformerless UPS systems in both the rectifier stage and at the load side inverter.

3.2 Two-level Voltage Source Converters

3.2.1 Operating principles of the Two-level Voltage Source Converters

The static switches are controlled by switching signals, S_{wk} that have two states 1 and 0 where k is the phase and 1 denotes closing of the upper switch and 0 is opening the upper switch.The Figure 3.2a shows the Two-level VSC.

$$S_{wk} = \begin{cases} 1 \\ 0 \end{cases} \tag{3.1}$$

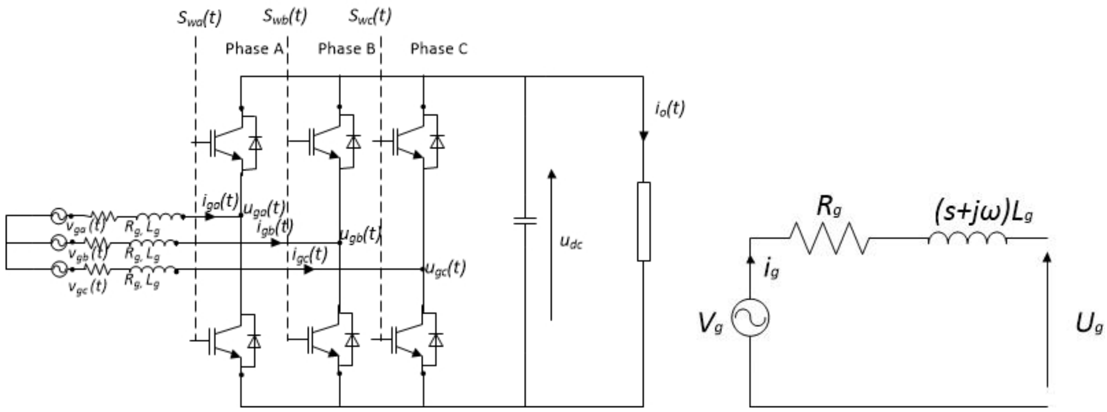

(a) (b)

Figure 3.2: a) Three phase Two-level VSC b) Equivalent Single phase Dynamic model of the VSC

Where,
V_g grid voltage
U_g converter voltage
R_g resistance of filter
L_g inductance of filter
i_g grid current

If ideal switches are used, taking KVL at each phase leg from Figure 3.2a

$$\begin{cases} L_g \frac{\mathrm{d}i_{ga}(t)}{\mathrm{d}t} = V_{ga}(t) - (R_g + j\omega L_g)i_{ga}(t) - u_{ga}(t) \\ L_g \frac{\mathrm{d}i_{gb}(t)}{\mathrm{d}t} = V_{gb}(t) - (R_g + j\omega L_g)i_{gb}(t) - u_{gb}(t) \\ L_g \frac{\mathrm{d}i_{gc}(t)}{\mathrm{d}t} = V_{gc}(t) - (R_g + j\omega L_g)i_{gc}(t) - u_{gc}(t) \end{cases} \tag{3.2}$$

In Figure 3.2aTaking KCL at the upper side of the load

$$C\frac{\mathrm{d}u_{dc}}{\mathrm{d}t} = i_{ga}(t)s_{wa} + i_{ga}(t)s_{wb} + i_{ga}(t)s_{wc} - i_0 \tag{3.3}$$

The equations above describe the behavior of the three phase converter in the *abc*-frame. It is necessary to make a *dq*- transformation where the reference sinusoidal will be a constant DC value and thus it will make it possible to use the conventional PI control to obtain the zero steady state error [18], (See Appendix A.1). Therefore in the *dq* frame the equations below are used per phase.

$$L_g\frac{\mathrm{d}i^{dq}}{\mathrm{d}t} = V^{dq} - R_g i^{dq} - j\omega L_g i^{dq} - u^{dq} \tag{3.4}$$

Re-arranging (3.4) above by making u^{dq} the subject

$$u^{dq} = V^{dq} - L_g\frac{\mathrm{d}i^{dq}}{\mathrm{d}t} - R_g i^{dq} - j\omega L_g i^{dq} \tag{3.5}$$

Separating the real and imaginary parts yields in (3.5)

$$u_d = V_d - L_g\frac{\mathrm{d}i_d}{\mathrm{d}t} - R_g i_d + \omega L_g i_d \tag{3.6}$$

$$u_q = V_q - L_g\frac{\mathrm{d}i_q}{\mathrm{d}t} - R_g i_q - \omega L_g i_q \tag{3.7}$$

$$C\frac{\mathrm{d}u_{dc}}{\mathrm{d}t} = \frac{3}{2}(i_d s_d + i_q s_q) - i_0 \tag{3.8}$$

3.2.2 Modulation strategies for Two-level Converters

i) Pulse Width Modulation [15]

Pulse Width Modulation (PWM) determines the switching patterns for the Two-level VSC to control its output voltage. In this modulation technique the reference voltage is compared with a triangular wave form to determine the switching sequence for the converter.
Where,
U_{dc} DC link Voltage
V_{ref} Magnitude of the reference voltage vector
φ Phase of the of the reference voltage

$$U^{(\alpha\beta)*}(t) = V_{ref}e^{j\varphi} \tag{3.9}$$

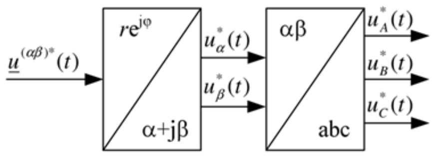

Figure 3.3: Transformation from $\alpha\beta$- to abc - frame

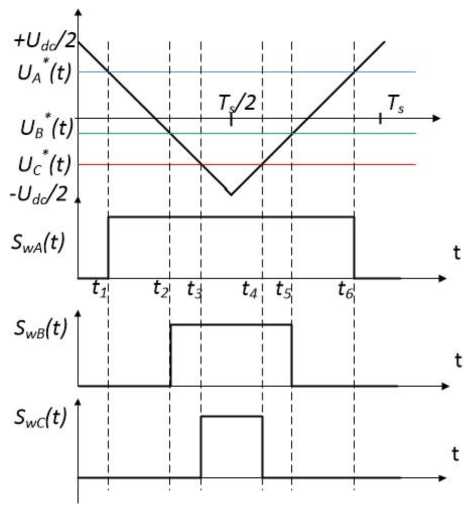

Figure 3.4: PWM Switching signals

When the triangular wave is higher than the reference voltage, then the upper switches will be turned off for the corresponding reference voltage in the phase leg and conversely when the triangular wave is lower than the reference voltage then the upper switches will conduct for that given reference voltage. The elements of the voltage vector show the corresponding switches that are conducting for a given phase at a given time. Element 1, denotes that the upper switch for that phase leg is conducting while Element 0, of voltage vector denotes that the upper switch of that phase leg is turned off and that the lower switch is the one conducting at that time.The switching pattern below for one switching cycle T_s are computed from Figure 3.4 [15].

ii) Space Vector Modulation (SVM)

In this type of modulation, the switching combinations of the converter are mapped in the $\alpha\beta$ plane [15] as seen in the Figure 3.5.

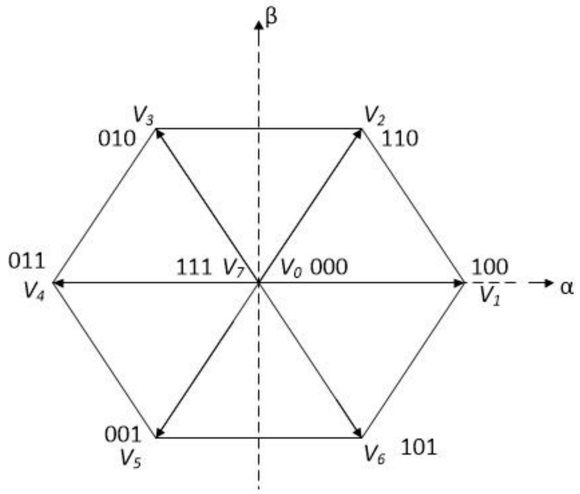

Figure 3.5: Switching Vectors for the VSC

If a voltage reference vector, V_{ref} is considered, then the dwell times t_0, t_1 and t_2 for the switches for one switching period T_s, in the vector diagram below in Figure 3.6 located in sector one can be obtained using using (3.10), (3.11) and (3.12) [15].

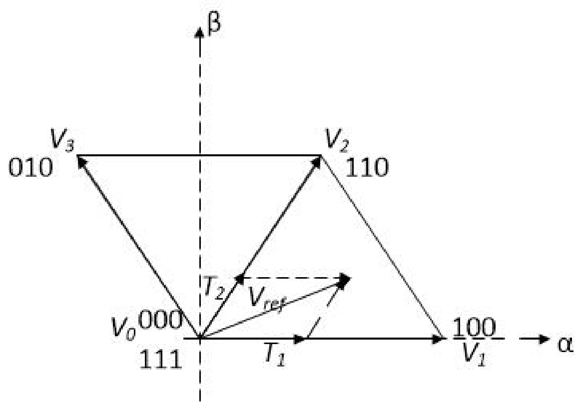

Figure 3.6: Space Vector Modulation (SVM)

$$t_1 = \frac{1}{2f_{sw}} \frac{V_{ref}}{U_{dc}} \left[\sqrt{\frac{3}{2}} (\cos\alpha - \frac{\sin\alpha}{\sqrt{2}}) \right] \tag{3.10}$$

$$t_2 = \frac{1}{2f_{sw}} \frac{V_{ref}}{U_{dc}} \sqrt{2} \tag{3.11}$$

$$t_0 = \frac{1}{2f_{sw}} - T_1 - T_2 \tag{3.12}$$

Where, $T_s = \frac{1}{f_{sw}}$ is the sampling time U_{dc} is the DC link Voltage V_{ref} is the magnitude of the reference voltage vector α is the phase of the of the reference voltage. If the reference vector is not in sector one, its rotated $60n$ to sector one and the same procedure is followed using (3.10), (3.11) and (3.12). The Switching patterns and durations are obtained by the expressions below;

$$\begin{bmatrix}0\\0\\0\end{bmatrix} \quad \begin{bmatrix}1\\0\\0\end{bmatrix} \quad \begin{bmatrix}1\\1\\0\end{bmatrix} \quad \begin{bmatrix}1\\1\\1\end{bmatrix} \quad \begin{bmatrix}1\\1\\0\end{bmatrix} \quad \begin{bmatrix}1\\0\\0\end{bmatrix} \quad \begin{bmatrix}0\\0\\0\end{bmatrix}$$

$\Delta T_1 = \frac{t_o}{2}$ $\Delta T_2 = t_1$ $\Delta T_3 = t_2$ $\Delta T_4 = t_0$ $\Delta T_5 = t_2$ $\Delta T_6 = t_1$ $\Delta T_7 = \frac{t_0}{2}$

3.2.3 Controller design for Two-level VSC

The traditional control of the Two-level VSC is used to control the UPS on the grid side. The load side converter is controlled in open loop and the SIMULINK model is shown in Figure A.7. The block diagram in Figure 3.7[19] is adopted from the control of a classical Two-level VSC presented in [19] with no modifications and is adapted to work as the rectifier part for the Two-level converter based UPS system. This controller makes use of a Phase-Locked Loop (PLL) that track the grid voltage angle, θ which is necessary to perform coordinate transformation [19]. The matrices to perform this kind of transformation can be found in Appendix A.1. The control strategy with double closed control loops is used in the d-q frame and it comprises of the current inner loop that considers error between the measured and the reference current as well as the voltage outer loop whose input is the error between the reference DC link voltage and the measured DC link voltages [18]. The basic control objective of this converter is to control the power factor to unity and also to control the DC Link voltage at the set reference.

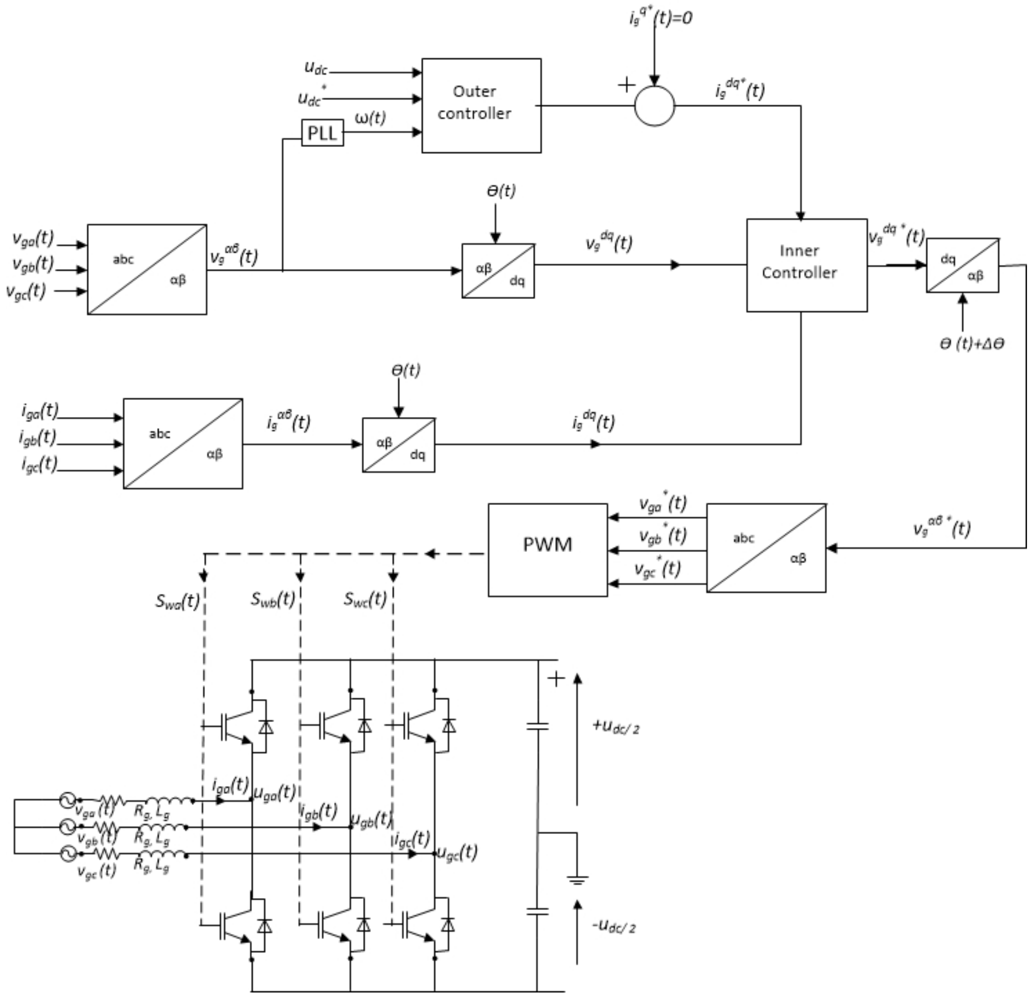

Figure 3.7: Overall control of the UPS Rectifier

3.3 Modular Multi-level Converters

3.3.1 Operating Principles of the MMC

The structure of the Modular Multi-level Converter with half-Bridge modules is seen in Figure 1.1. It consists of three arms with $2N$ sub-modules per phase leg. It is symmetrical and there are N sub-modules in the positive, as well as the negative arm of the phase leg. The electric model for a single phase of the VSC is shown in the Figure 3.8 below. To understand the overall operation of the MMC VSC, it is pertinent to understand the operation its single phase first.

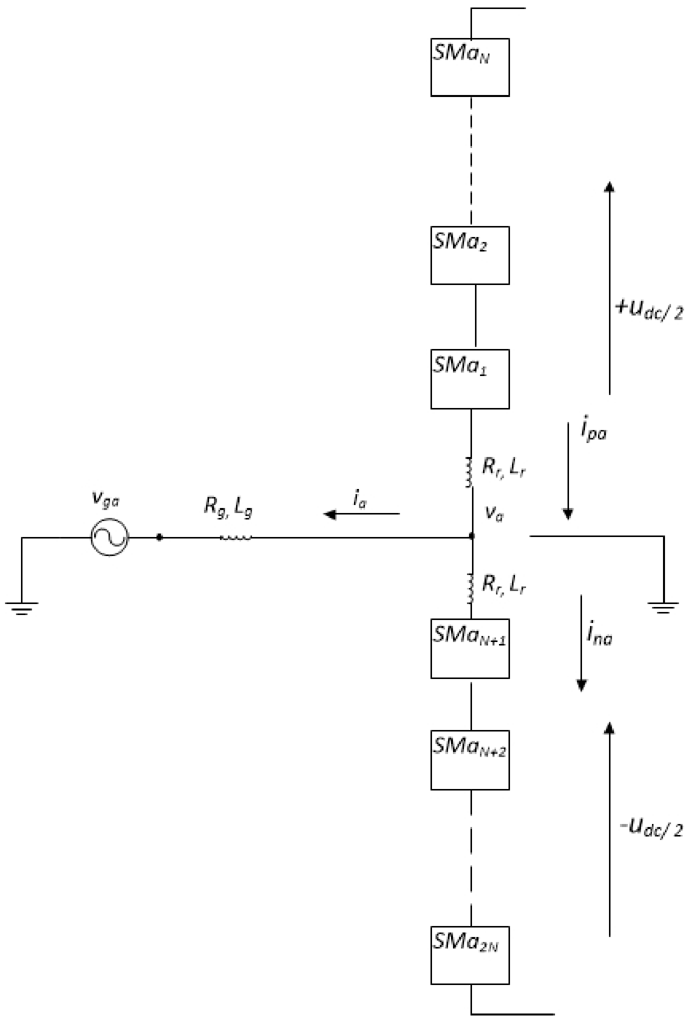

Figure 3.8: Modular Multi-level Converter

Using KCL at the node connecting the positive and negative arms of phase leg a,

$$i_a = i_{pa} - i_{na} \tag{3.13}$$

Using KVL at the upper loop

$$0 = \frac{U_{dc}}{2} - u_{m1} - u_{m2} - \cdots u_{mN} - L_r \frac{\mathrm{d}i_{pa}(t)}{\mathrm{d}t} - R_r i_{pa} - v_a \tag{3.14}$$

where u_{mN} is the capacitor voltage of cell located at position N in the phase leg.

$$0 = \frac{U_{dc}}{2} - \sum_{j=1}^{N} u_{mj} - L_r \frac{\mathrm{d}i_{pa}(t)}{\mathrm{d}t} - R_r i_{pa} - v_a \tag{3.15}$$

Consequently, for the Lower Loop

$$0 = \frac{U_{dc}}{2} - \sum_{j=N+1}^{2N} u_{mj} - L_r \frac{\mathrm{d}i_{na}(t)}{\mathrm{d}t} - R_r i_{na} + v_a \tag{3.16}$$

Subtracting (3.15) from (3.16) yields (3.17),

$$\sum_{j=1}^{N} u_{mj} - \sum_{j=N+1}^{2N} u_{mj} = 2v_a - L_r \frac{\mathrm{d}i_{na}(t)}{\mathrm{d}t} - R_r i_{na} + L_r \frac{\mathrm{d}i_{pa}(t)}{\mathrm{d}t} + R_r i_{pa} \tag{3.17}$$

$$v_a = \frac{1}{2}\left[\sum_{j=1}^{N} u_{mj} - \sum_{j=N+1}^{2N} u_{mj}\right] - \frac{1}{2}\left[L_r \frac{\mathrm{d}i_{pa}}{\mathrm{d}t} - L_r \frac{\mathrm{d}i_{na}}{\mathrm{d}t} + R_r\left(i_{pa} - i_{na}\right)\right] \tag{3.18}$$

Substituting (3.13) into (3.18) yields (3.19) below.

$$v_a = \frac{1}{2}\left[\sum_{j=1}^{N} u_{mj} - \sum_{j=N+1}^{2N} u_{mj}\right] - \frac{1}{2}\left[L_r \frac{\mathrm{d}i_a}{\mathrm{d}t} + R_r i_a\right] \tag{3.19}$$

Adding (3.15) and (3.16), we obtain,

$$u_{dc} - \left[\sum_{j=1}^{N} u_{mj} + \sum_{j=N+1}^{2N} u_{mj}\right] = L_r \frac{\mathrm{d}\left(i_{pa} + i_{na}\right)}{\mathrm{d}t} + R_r\left(i_{pa} + i_{na}\right) \tag{3.20}$$

From (3.20) above, if the arm is to be controlled to be DC, then the sum total of the currents in the positive and negative arms of the phase leg is DC [20].

$$i_{pa} + i_{na} = i_{dc} \tag{3.21}$$

Therefore (3.20) becomes,

$$u_{dc} - \left[\sum_{j=1}^{N} u_{mj} + \sum_{j=N+1}^{2N} u_{mj} \right] = L_r \frac{\mathrm{d}\, i_{dc}}{\mathrm{d}t} + R_r i_{dc} \tag{3.22}$$

For UPS system applications, In the rectifier mode of operation, the sum of the sub-module voltage will be controlled to be greater than the DC Link voltage to enable power flow from the AC side to the DC side [20]

$$\left[\sum_{j=1}^{N} u_{mj} + \sum_{j=N+1}^{2N} u_{mj} \right] \geq u_{dc} \tag{3.23}$$

And conversely, when the sum total of the sub-module voltages is less that the DC link, then power will flow from the DC side to the AC side and now the converter will be operating as an inverter.

Circulating Currents

The presence of circulating currents in the phase legs of the converter is one of the significant differences between Two-level VSCs and Modular Multi-level Converters. These currents circulate through the phase legs of the MMC without causing modifications to the AC Voltages. If we consider phase leg a, the circulating currents i_{diff} can be expressed in (3.24) and (3.25)

$$i_{pa} = i_{diff} + \frac{i_a}{2} \tag{3.24}$$

$$i_{na} = i_{diff} - \frac{i_a}{2} \tag{3.25}$$

Comparing (3.24), (3.25) and (3.13), we get

$$i_{diff} = \frac{i_{pa} + i_{na}}{2} \tag{3.26}$$

Thus, the circulating current is half of the sum of the positive arm current and the negative arm current per phase leg. These circulating currents have significant second order harmonics that could increase the rating of the semiconductors components if not controlled. The concept of circulating currents is analyzed and proved in [20].

Modulation strategy for the MMC

Pulse width Modulation with vertically shifted carriers is used for the MMC. In this modulation, the reference signal is compared with the triangular carrier waves to generate the switching signals. In the MMC, with m voltage levels, (m-1) triangular carriers with the same frequency that are in phase are arranged vertically one above the other [21]. The Figure 3.9 shows the 10 triangular carriers at 1kHz frequency compared to a sinusoidal modulating wave at 50 Hz in vertically shifted PWM.

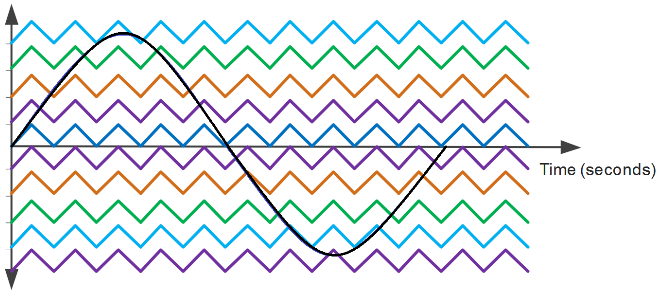

Figure 3.9: Carrier arrangement for vertically shifted PWM

3.3.2 Controller Design for Modular Multi-level Converters

Current Controller design

The equivalent dynamic model of the MMC with inductor filter is similar to that of the Two-level VSC in the synchronous rotating frame described in Figure 3.2b. The model of the single phase model of the MMC is shown in the Figure 3.10 below.

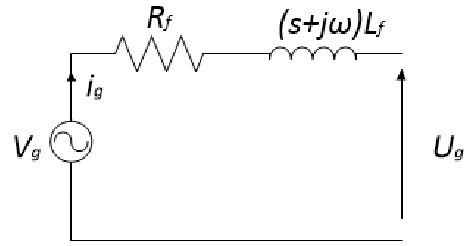

Figure 3.10: Equivalent Dynamic model of the MMC

Where,
R_r Arm resistance
L_r Arm inductance
R_f resistance of filter where $R_f = R_g + \frac{R_r}{2}$
L_f inductance of filter where $L_f = L_g + \frac{L_r}{2}$

Owing to the similarity in the circuit structure of the equivalent dynamic model of the MMC in Figure 3.10 and the Two-level VSC shown in Figure 3.2b, the basic control strategy of the MMC will be adopted from that of the traditional Two-level VSCs. However there is additional voltage balancing of the sub-modules per phase leg of the MMC [5]. The controller for the MMC UPS is based on the internal model control (IMC) theory basics presented in [22] where the controller is designed based on the parameters of the plant model and the bandwidth that is desired in closed loop.

The Figure 3.11 shows the control structure based on IMC

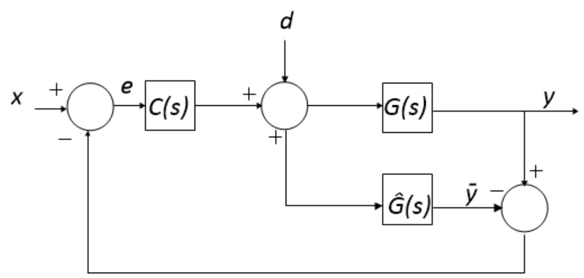

Figure 3.11: Structure of Internal Model Control system

where,

$G(s)$ plant
$\widehat{G}\,(s)$ plant model
$C(s)$ IMC controller
x input
y output
d disturbance
The control structure in Figure 3.11 can be simplified as shown in the Figure 3.12 , which is depicted as the classical control system. See [22] .

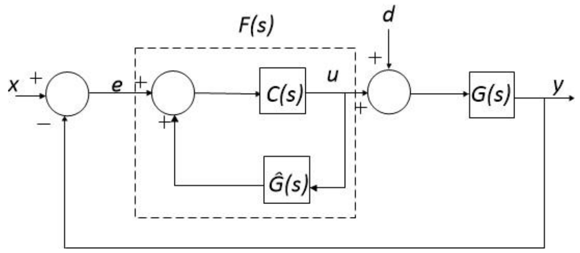

Figure 3.12: Re-arranged Structure of Internal Model Control system

Where the transfer function, $F(s)$ of the controller with input e and output u is given by the expression in (3.27).

$$F(s) = \frac{C(s)}{1 - C(s)\widehat{G}(s)} = \frac{\alpha^n}{(s+\alpha)^n - \alpha^n}\widehat{G}^{-1}(s) \tag{3.27}$$

For a first order system the n=1, and (3.27) becomes;

$$F(s) = \frac{\alpha}{s}\widehat{G}^{-1}(s) \tag{3.28}$$

(3.29) relates the converter voltage and the grid voltage in the in the in the synchronous rotating frame from Figure 3.10

$$sL_f = V_g^{dq} - (R_f + j\omega L_f)i_g^{dq} - u_g^{dq} \tag{3.29}$$

$$i_g^{dq} = \frac{V_g^{dq} - u_g^{dq}}{R_f + sL_f + j\omega L_f} \tag{3.30}$$

Thus, the transfer function, $G(s)$ that relates u^{dq} and i^{dq} in the process model is obtained by re-arranging and finding the laplace of (3.4) shown below in (3.29).

$$G(s) = \frac{-1}{R_f + sL_f + j\omega L_f} \tag{3.31}$$

Active damping and current decoupling are introduced to speed up grid voltage disturbance response by selecting u_g as shown in (3.32).

$$u_g^{dq} = u_g^{\prime dq} - (R_a - j\omega L_f) i_g^{dq} \tag{3.32}$$

Where R_a the damping resistance

Substituting (3.32) into (3.31), we obtain

$$G'(s) = \frac{-G(s)}{1 + (R_a - j\omega L_f)\, G(s)} = \frac{1}{R_f + R_a + sL_f} \tag{3.33}$$

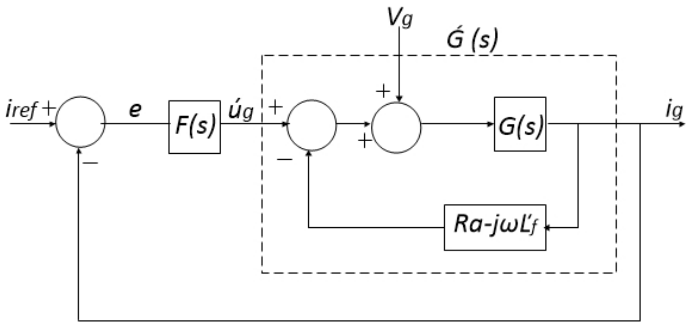

Figure 3.13: Grid current control with active damping

The Figure 3.13 shows a control system structure for grid control with inner current decoupling and active damping [22] , the current controller $F(s)$ is given by (3.34).

$$F(s) = \frac{\alpha_c}{s} G'(s)^{-1} = \alpha_c L'_f + \frac{\alpha_c}{s}(R_f + R_a) \tag{3.34}$$

R_f is designed to be very small [22]. From the (3.34),

$$k_{pc} = \alpha_c L'_f \tag{3.35}$$

$$k_{ic} = \alpha_c (R_f + R_a) \tag{3.36}$$

Where α_c is the bandwidth of the current controller and It should be chosen less than a tenth of the sampling frequency

$$\alpha_c < \frac{\omega_s}{10} \tag{3.37}$$

DC Link Voltage Controller design

The control system structure for the DC link voltage of the grid connected VSC can be achieved by feedback linearization [22]. This is because the DC link voltage has a non-linear relationship with the d-axis current, therefore the VSC cannot be controlled by the traditional linear PI controller [18]. In a UPS system there exists energy storage in the DC link such as Lead Acid batteries. A smoothing Capacitor is used to maintain a stable DC link voltage.DC voltage dynamics can be described by (3.38).

$$C\frac{\mathrm{d}\ v_{dc}}{\mathrm{d}t} = i_g - i_l \tag{3.38}$$

Where,
i_g current from the grid
i_l current to load
C capacitance of DC link capacitor
v_{dc} DC link voltage

From the principle of power balancing,

$$P_g = v_{dc}(C\frac{\mathrm{d}\ v_{dc}}{\mathrm{d}t} + i_l) \tag{3.39}$$

thus,

$$P_g = v_{dc}C\frac{\mathrm{d}\ v_{dc}}{\mathrm{d}t} + P_l \tag{3.40}$$

Where, P_g is the power from the grid and P_l is the power to load

(3.41) can be written in the form below.

$$\frac{1}{2}C\frac{\mathrm{d}\ v_{dc}^2}{\mathrm{d}t} = P_g - P_l \tag{3.41}$$

If,

$$W = v_{dc}^2 \tag{3.42}$$

then substituting (3.42) in (3.41), we obtain (3.43)

$$\frac{1}{2}C\frac{\mathrm{d}\ W}{\mathrm{d}t} = P_g - P_l \tag{3.43}$$

(3.43) represents the energy dynamics of the DC link voltage, where the DC link voltage has a square relationship with the power transferred on the DC link [22].

$$\frac{1}{2}C\frac{\mathrm{d}\,W}{\mathrm{d}t} = 3v_g i_d - P_l \tag{3.44}$$

Taking the Laplace transform on both sides of (3.44).

$$\frac{1}{2}CsW = 3v_g i_d - P_l \tag{3.45}$$

$$\frac{W}{i_d} = \frac{6v_g - P_l}{sC} \tag{3.46}$$

For near unity power factor operation of the voltage source converter [18].

$$i_{dq} = i_d \tag{3.47}$$

The transfer function, $G(s)$ that relates W and i_d in the process model is obtained as seen in (3.48) from (3.46).

$$G(s) = \frac{6v_g}{sC} \tag{3.48}$$

An inner loop for active damping is introduced since the transfer function has a pole at the origin [18] by setting i_d to be as shown in the (3.49) below.

$$i_d = i'_d - G_a W \tag{3.49}$$

Where G_a is the active conductance. Substituting (3.49) into (3.48), we obtain

$$G'(s) = \frac{6v_g}{sC + 6G_a V_g} \tag{3.50}$$

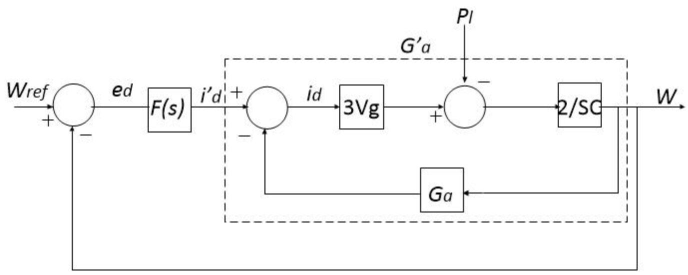

Figure 3.14: DC link voltage control with active damping

The Figure 3.14 shows a control system structure for DC link voltage control with active damping in the inner feedback loop [22], the DC voltage controller $F(s)$ is given by (3.51).

$$F(s) = \frac{\alpha_v}{s} G'(s)^{-1} = \frac{\alpha_v C}{6v_g} G'(s) + \frac{G_a \alpha_v}{6v_g} \tag{3.51}$$

Thus,

$$k_{iv} = G_a \alpha_v \tag{3.52}$$

Where α_v is the bandwidth of the voltage controller and It should be chosen less that of the current controller, ($\alpha_v < \alpha_c$). G_a is obtained by placing the pole of $G'(s)$ at $-\alpha_v$ in (3.49). This is done in a bid to ensure that the inner feedback loop is as fast as the closed loop system [22].

Thus,

$$G_a = \frac{\alpha_v C}{6v_g} \tag{3.53}$$

Putting (3.53) into (3.52) we obtain,

$$k_{iv} = \frac{\alpha_v^2 C}{6v_g} \tag{3.54}$$

and from (3.53)

$$k_{pv} = \frac{\alpha_v}{6v_g} \tag{3.55}$$

Voltage balancing of sub-modules

This voltage balancing control is based on the sorting algorithm that puts into consideration a combination the magnitude of the sub-module capacitor voltage at that time and the direction of the arm current to determine the sub-module that should be switched on.

The sub-module with the lowest average voltage across its capacitor is inserted in ascending order in the arm, this is provided the current through that arm is charging the capacitors [23] and also on the contrally, the sub-module with the highest average voltage across its capacitor is inserted in, in descending order in the arm when the current through that arm is discharging the capacitors [23]. The module capacitor voltage balancing algorithm described below is based on the sorting algorithm from [5] and applied to balance the module capacitor voltages for the MMC converters.

3.3.3 DC Link capacitor Sizing

The DC link voltage V_{dc} should be at least be the amplitude of the AC input line voltage V_{nom} and it is given by the expression in (3.56)

$$V_{dc} \geq \frac{2\sqrt{2}V_{nom}}{\sqrt{3}} \tag{3.56}$$

When selecting the DC link capacitor for the UPS, the time constant τ, is selected and used to compute the DC link capacitance C_{dc} based on (3.57) below.

$$\tau = \frac{C_{dc}V_{dc}^2}{2S_{nom}} \tag{3.57}$$

Where, S_{nom} is the rated power. The motivation behind (3.57) is that the capacitor should have the ability to store energy equivalent to the power requirements of the rated load for a time period, τ seconds.

4

Simulation and Analysis of results

4.1 Conventional UPS system with Two-level Based converters

The Two-level UPS system was implemented using appropriate Matlab/SIMULINK blocks from the Powersys Library [24]. The Figure 4.1 shows the circuit for the UPS connected to a 400V LV supply. The static transfer switches facilitate the transfer of the load to the batteries during emergency operation of the UPS. The UPS circuit consists of a battery pack that is mounted in the DC link through a DC-DC converter.

The battery model that is used in the simulation is the Lead Acid model that was taken from the Matlab/SIMULINK library with appropriate parameters.The motivation behind the choice is that the deep cycle lead acid batteries are commonly used for UPS applications since they allow maximum utilization of the capacity of the battery.

The circuit in Figure 4.1 consist of a DC-DC converter in the DC link which is a buck-boost converter. Through appropriate input signals sent to the DC-DC converter, it decides to charge or discharge the batteries by acting as a boost converter during discharge and as a buck converter during the charging periods. The proposed input signals to the DC-Dc converter include but are not limited to; the SOC of the batteries, preference of the power source in case there are renewable energy sources and the detection of disturbances in the grid supply. This DC-DC converter has been included on the circuit diagram to show completeness of the UPS system but was not implemented in the simulation model. rather ideal switches were used to switch to the UPS battery operation. The simulation model for the UPS system is shown in Figure A.5 and the Table 4.1 shows the Parameters of the UPS that were used for the simulation.

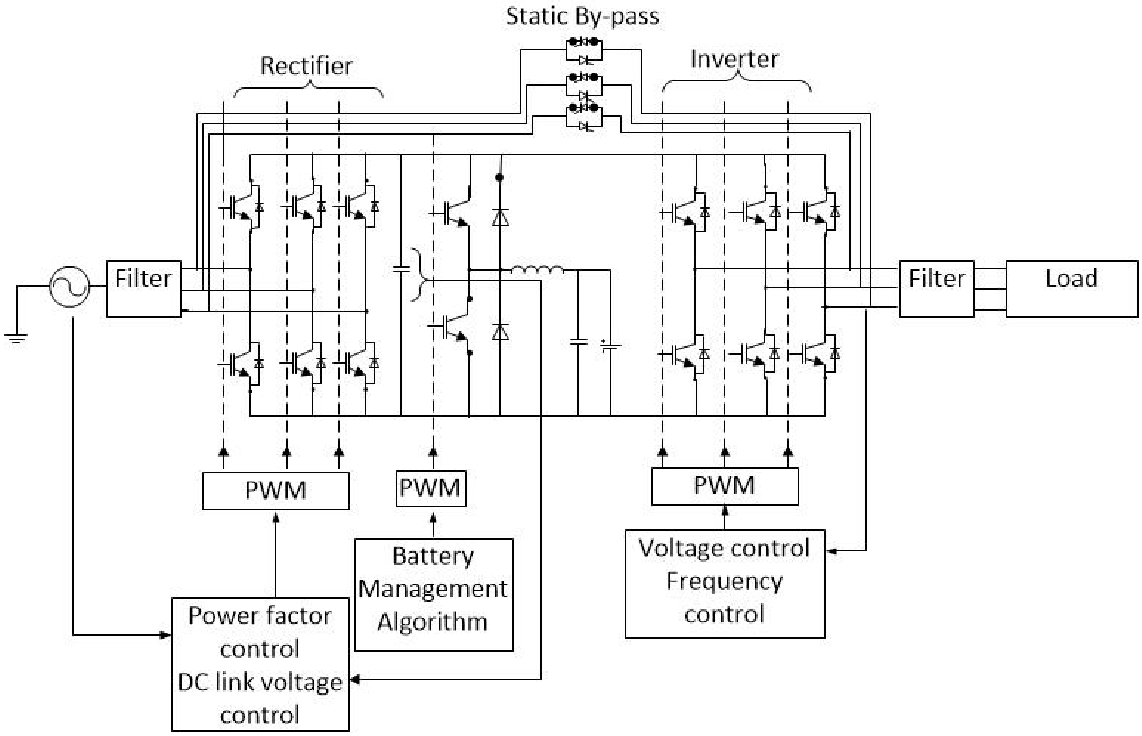

Figure 4.1: Simulation model for Two-level VSC based UPS System

Table 4.1: Two-level VSC based UPS Simulation Parameters

General Parameters	Symbol	Value
Nominal Voltage	V_{nom}	$400V$
Nominal Power	S_{nom}	$45kVA$
Nominal Frequency	f_{nom}	$50Hz$
Carrier Frequency	f_{sw}	$2kHz$
Filter inductance	L_f	$5mH$
Filter Capacitance	C_f	$159\mu F$
Leakage resistance	R_g	1Ω
DC link Voltage	V_{dc}	$653V$
DC link Capacitance	C_{dc}	$1525\mu F$
Rectifier Parameters	**Symbol**	**Value**
Proportional of current Controller	k_{pc}	0.5
Integral of current Controller	k_{ic}	100
Proportional of outer Controller	k_{pv}	$1.44X10^{-2}$
Integral of Outer Controller	k_{iv}	$4.4X10^{-4}$

A. Two-level UPS Performance under Load with resistive-inductive Loads

The UPS was simulated with load of 0.75 p.f leading that was connected to the output of the UPS. It is observed that the output voltage in Figure 4.2b and the output current 4.2d shows that the wave forms are not in phase as a result of non unity power factor operation. However because of the connection of the load to the grid through the UPS system, the UPS presents a unity power factor to the upstream power distribution system. This can be observed by a comparision between the Figures 4.2a and 4.2c

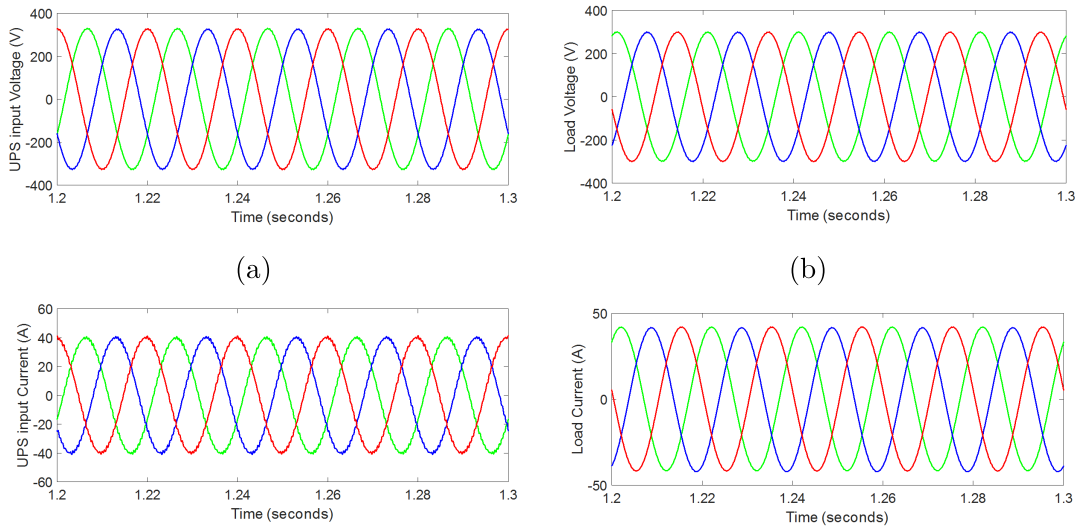

(a) (b)

(c) (d)

Figure 4.2: a) UPS input voltage b) Load Voltage c) UPS input current and d) Load current with inductive-resistive load

The Two-level based UPS system had the following output square voltage wave form at its inverter as shown in Figure 4.3 below.

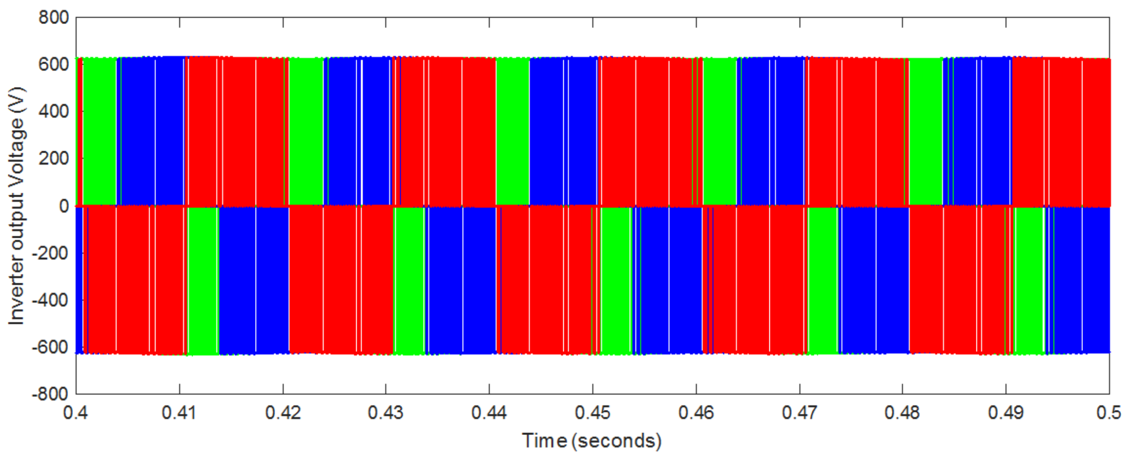

Figure 4.3: Two-level VSC based UPS Inverter output Voltage

Harmonic analysis was performed by computing the FFTfor the first 140 harmonics of the UPS output Voltage using powergui tool in matlab/SIMULINK and it indicated that there were harmonics around multiples of the switching frequency and a THD of 69.35% in the voltage output of the UPS at the inverter side. See Figure 4.4 below.

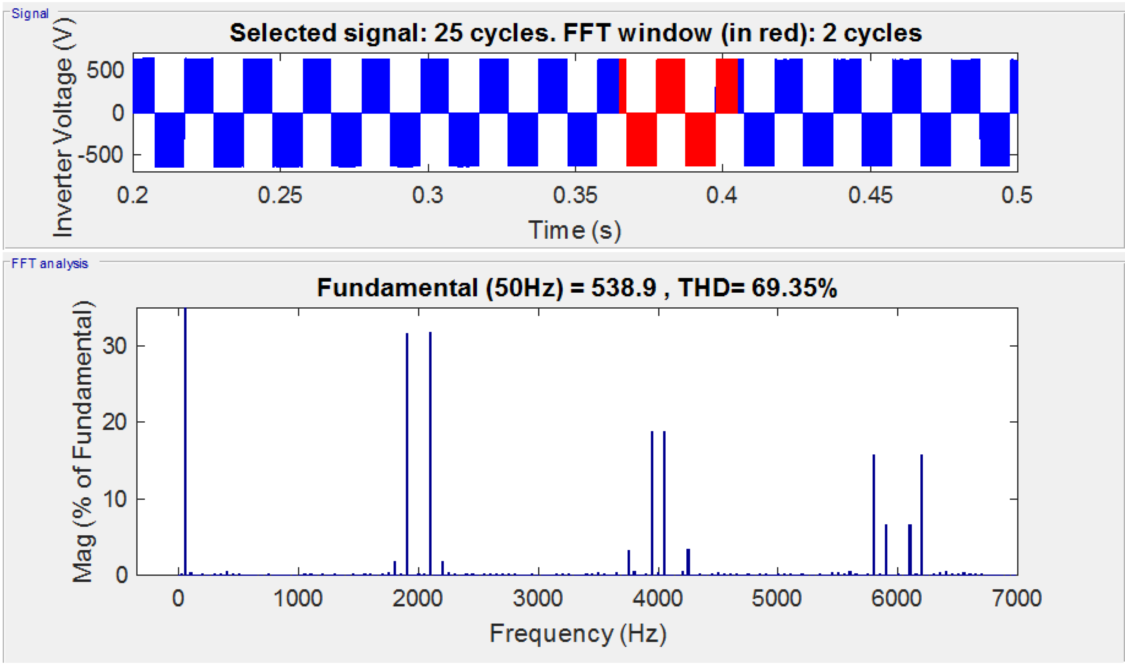

Figure 4.4: Harmonic analysis of the Two-level VSC UPS Inverter output voltage

B. Performance with Non-linear Loads

In most applications where UPS systems are used, there a a number of Non-linear loads such as power supplies for IT or hospital equipment. With this background the UPS system was simulated for during the operation with a non-linear load. The non-linear load consisted of a full bridge uncontrolled rectifier circuit with a resistive load. The Figure 4.5 below shows the grid voltage and currents for the UPS system.

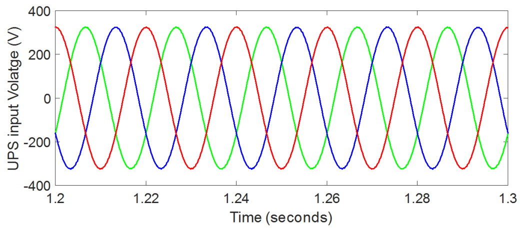

(a)

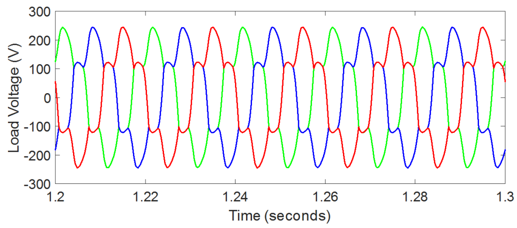

(b)

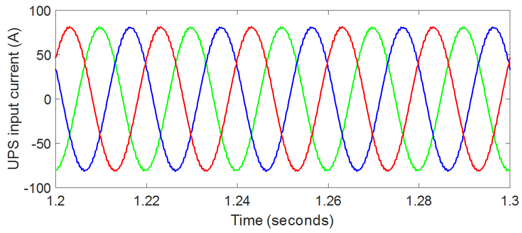

(c)

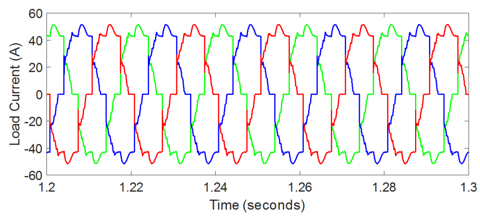

(d)

Figure 4.5: a) UPS input voltage b) Load Voltage c) UPS input current and d) Load current with Non linear load

It is observed that the current wave forms are distorted at the load side as shown in Figure 4.5d. The distortion is a sign that the wave forms contain harmonics that if not filtered can create voltage distortions in the distribution systems and nearby loads. Because of of the operation of the UPS system, there are no distortion in the input current as well as the input voltage as seen in Figure 4.5a and Figure 4.5c. In addition the grid current and Voltage are in phase that implies that the UPS system is operating at unity power factor.

C. UPS under Emergency operation

During a power disturbance or an interruption at the grid side, the UPS system will be able to continually supply the load through its batteries. In this simulation the battery model used is the Lead Acid battery from Matlab/SIMULINK library. The batteries are connected in the DC link of the UPS system and they ensure a continuous supply of power to an active power load connected to the output of the UPS.

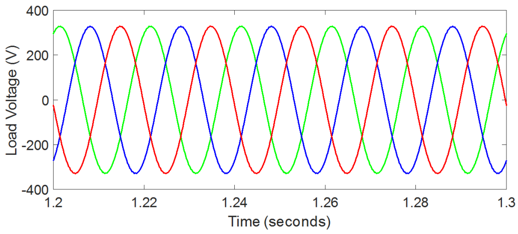

(a)

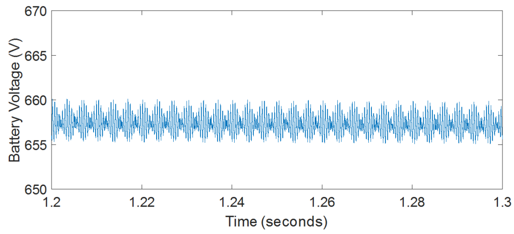

(b)

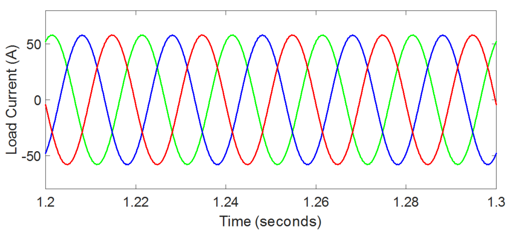

(c)

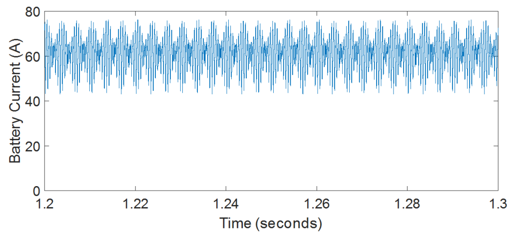

(d)

Figure 4.6: a) UPS input voltage b) Battery Voltage c) UPS input current and d) Battery current during emergency UPS operation

The battery supply active power to enable continuous supply to the load during an interruption or power disturbance from the grid supply. The lead acid battery maintains a stable DC link voltage and current during its operation as seen from Figure 4.6b and Figure 4.5d

4.2 Simulation Model for the MMC based UPS system

The circuit for the MV MMC based UPS system consists of two MMCs in a back to back arrangement with storage mounted in the DC link. It has static transfer switches to enable to transfer the load from the mains supply to the batteries under emergency operation of the UPS system. In the DC link, we find a DC-DC converter with the battery management algorithm that enables efficient charging and discharging of the batteries as shown in the Figure 4.7 below. The static transfer switches were not included for the simulation.

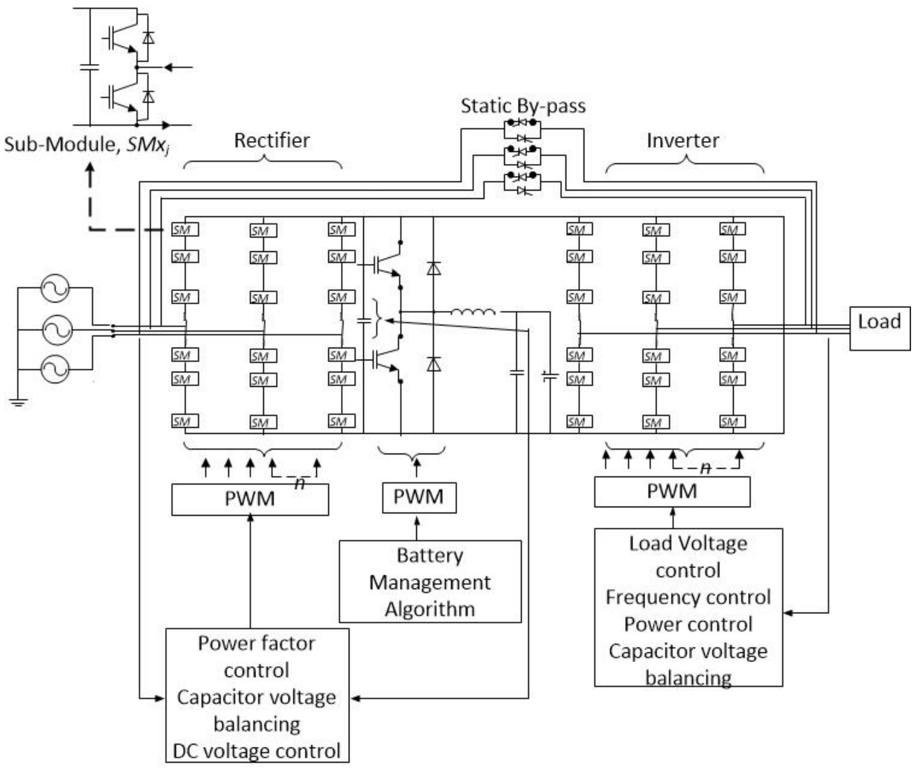

Figure 4.7: Simulation model for the MMC based UPS System

Where $N = 10$ and $x = (a, b, c)$ for $(1 < j < 20)$

The MMC UPS system was implemented in Matlab/SIMULINK with PLECS Blocksets since MMC modules and controllers in PLECS can easily be implemented by specifying the number of cells per arm of the MMC without the need to extend the physical model with more cells and connection as compared to Matlab/SIMULINK and other tools. Other simulation environments may necessitate making physical connections of individual cells and this increases the complexity of the simulation especially when dealing with an MMC with many cells. The simulation made use of IGBT Half bridges from the PLECS power module library in the switched configuration since the MMC UPS consisted of only 10 sub-modules per arm and therefore a relatively fast simulation could achieved using the configuration. The UPS model is a modification of the HVDC model in [25], with appropriate changes made in the circuit structure and control of the model to function as a UPS at medium voltage, 10kV. The control objectives for the MMC rectifier shown in Figure A.3 are to regulate the DC link voltage and also achieve unity power at the UPS input. For the inverter side where the load is connected as shown in Figure A.4, the control objectives are to control the output voltage.

The simplest grid filter is the L-filter which consists of line inductors per phase mounted between the converter and the grid [26] to provide smoothing and thereby reduce the grid current ripple. The L-filter was selected for the implementation of the MMC UPS system. The motivation for the choice of this L-filter is that it is a simple filter than can suitably be used at higher switching frequencies. The filter inductance, L_f was determined by running the simulation with the arm inductance, L_r fixed at 5mH and a small grid inductor of 1mH. Using the powergui tool in Matlab/SIMULINK, the THD in line current was computed as 18.9% . The line inductance, L_g was incremented in steps of 0.5mH for each proceeding simulation until a THD of 1.5% was obtained in the grid current. The value of the L_g was recorded as 5mH. The filter inductance was computed from the expression $L_f = L_g + \frac{L_r}{2}$. To obtain smoother line current wave forms that have very low THD, a higher switching frequency should be used or a bigger line filter. However, a high switching frequency will result into more losses in the valves. The switching frequency of the Two-level VSC is dependent on the rated power of the converter [26]. The higher the power rating, the lower the switching frequency should be. For high power UPS applications, the switching frequency for the Two-level VSC could be as low as 1kHz [26] [27]. In this thesis, a switching frequency of 2kHz is chosen for the Two-level VSC based UPS system. For the MMC based UPS system, a lower but comparable actual switching frequency of 1kHz was used that is equivalent to an effective switching frequency of 10kHz for the particular case of the MMC for a higher power application. Appropriate control parameters were computed for the UPS converter operation based on the theory in *Chapter* 3 of this thesis and tabulated in the Table 4.2.The MMC UPS performance was simulated for various operating scenarios that are described herein thereafter.

Table 4.2: MMC based UPS Simulation Parameters

General Parameters	**Symbol**	**Value**
Nominal Voltage	V_{nom}	$10kV$
Nominal Power	S_{nom}	$15MVA$
Nominal Frequency	f_{nom}	$50Hz$
Carrier Frequency	f_{sw}	$1000Hz$
Submodules per Arm	N	10 Cells
Filter Inductance	L_f	$7.5mH$
Arm Resistance	R_r	0.1Ω
Leakage Resistance	R_g	0.1Ω
DC link Voltage	V_{dc}	$16.4kV$
DC link Capacitance	C_{dc}	$500\mu F$
Rectifier Parameters	**Symbol**	**Value**
Proportional of Inner current Controller	k_{pc}	6.500x10^{-1}
Integral of Inner current Controller	k_{ic}	6.500x10^{1}
Proportional of Outer Controller	k_{pv}	2.357x10^{-7}
Integral of Outer Controller	k_{iv}	4.714x10^{-6}

A. MMC UPS Performance with Unbalanced loads

Load balancing is when the current is equally shared among the phases at the customer premises. The simulation was done and an unbalanced load with the blue phase carrying only half of the load as compared to other phases as shown in Figure 4.8c. It was observed that at the UPS input there was a load balance as seen in Figure 4.8d. Figure 4.8f shows the overall DC link voltage that is evenly shared among the cells in the positive arm of the MMC as shown in the Figure4.8f. The Figure 4.8 below shows the UPS operation under unbalanced load conditions. The load in this scenario consists of three single phase resistive loads where the power consumption of the blue phase is 50% less than in the other phases at the UPS output. Observations in the supply to the UPS indicate that there is a load balance and unity power factor operation as seen at the MMC base UPS input in Figure 4.8a and Figure 4.8c .

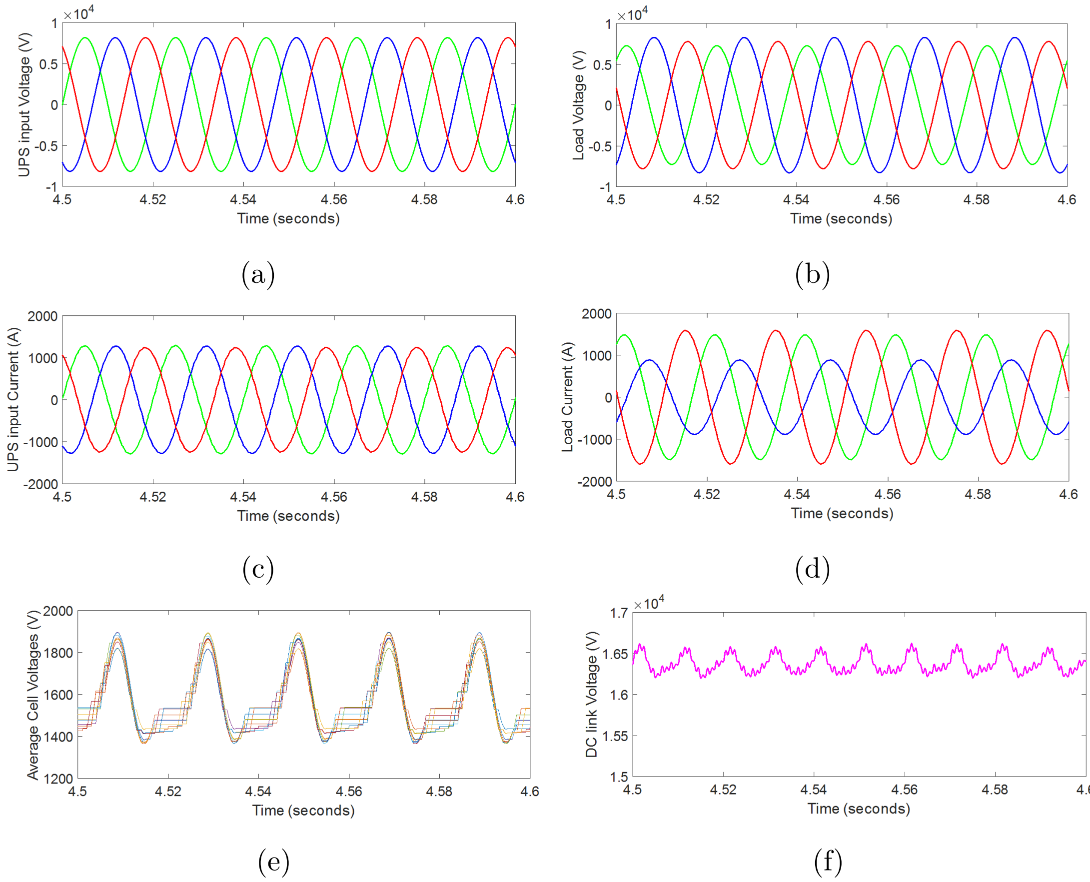

Figure 4.8: a) MMC UPS input voltage b) Load Voltage c) MMC UPS input current and d) Load current e) Average Cell Voltages f) DC link Voltage under unbalanced load conditions

This result indicates that if the UPS system is used, the electric panel connected to the grid will be balanced, the electric current is shared more evenly among the phases and this cancels out the neutral current. In a poorly balanced network for example when one load is more loaded as compared to the other the neutral carries large currents.

The MMC converter stair case output voltage waveform in Figure 4.9, is close to a sinusoidal waveform as compared to the Two-level VSC which has square wave forms. Because of this reason it is observed that in relation to the power rating of the MMC UPS system, it has smaller filter requirements compared to the Two-level UPS system to achieve the same value of THD in both voltage and current.

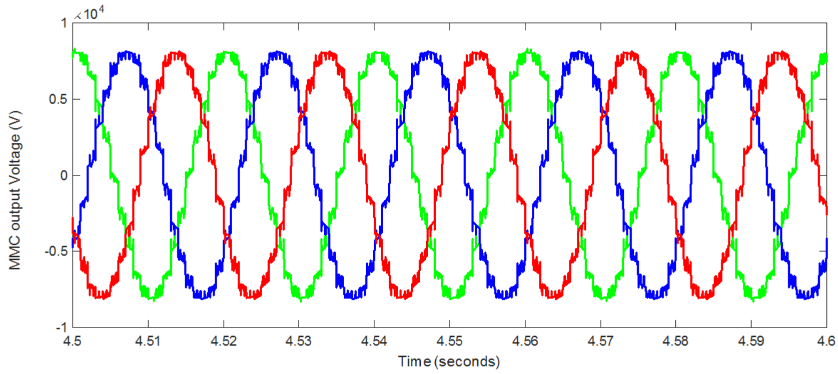

Figure 4.9: MMC based UPS Inverter output Voltage

B. MMC UPS Performance with Non-linear loads

Most installations where UPS systems are installed house a number of non-linear loads such as DC power supplies for DC loads with bridge rectifier circuits for example DC motor drives and computer equipment. These non-linear loads in absence of a UPS system reduce the quality of the supply current. The non linear load in this simulation consisted of three phase full bridge uncontrolled rectifier circuit each a resistive load.

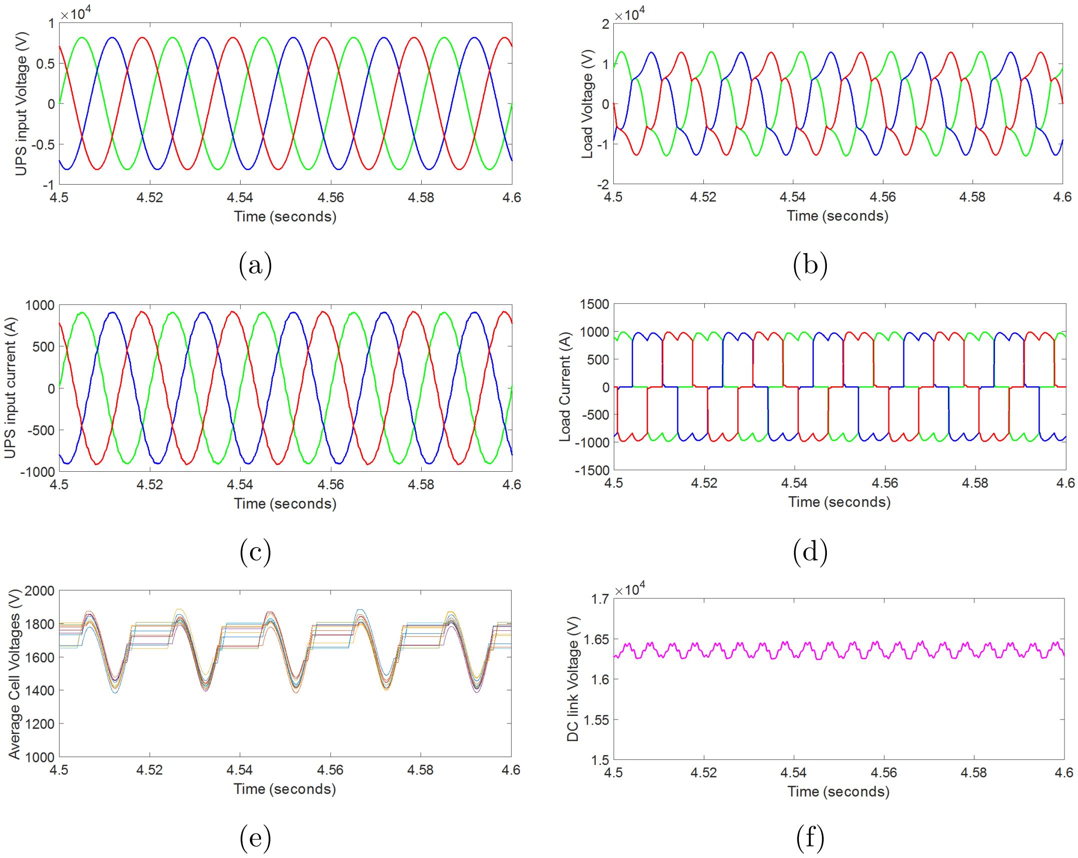

Figure 4.10: a) MMC UPS input voltage b) Load Voltage c) MMC UPS input current and d) Load current e) Average Cell Voltages f) DC link Voltage with non-linear load

It is observed that the current wave forms are distorted at the load side as shown in Figure 4.10d. The distortion is a sign that the wave forms contain harmonics that if not filtered can create voltage distortions in the distribution systems and nearby loads. Because of of the operation of the UPS system, there are no distortions in the input current as well as the input voltage as seen in Figure 4.10a and Figure 4.10a. The grid current and Voltage are in phase that shows that the UPS system is operating at unity power factor. The overall DC link voltage in Figure 4.10f is also well distributed in the cells of the positive arm of the MMC UPS inverter as shown in the Figure4.10e

C. MMC UPS Performance with inductive-resistive load

The UPS is loaded with an inductive-resistive load with a power factor of 0.7 lagging at its output as shown by the wave forms in Figure 4.11b and Figure 4.11d. Observation of the UPS input shows that the current and the voltage are in phase as seen in Figure 4.11a and Figure 4.11c. This implies that the UPS is operating at unity power factor at its input.

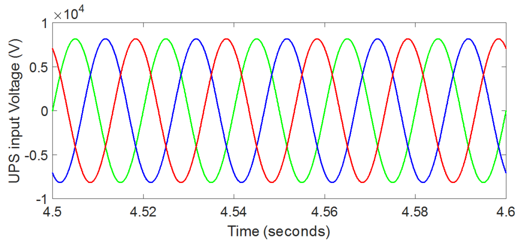

(a)

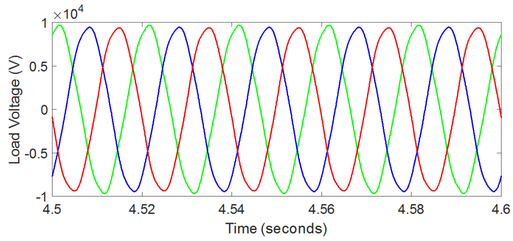

(b)

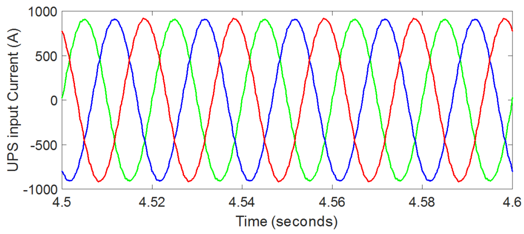

(c)

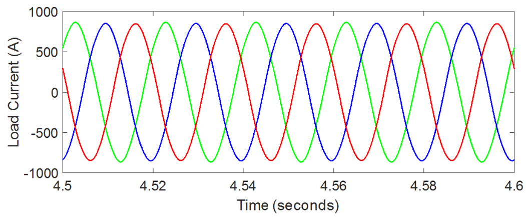

(d)

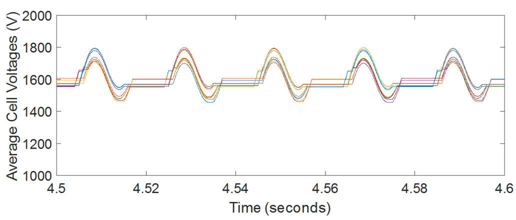

(e)

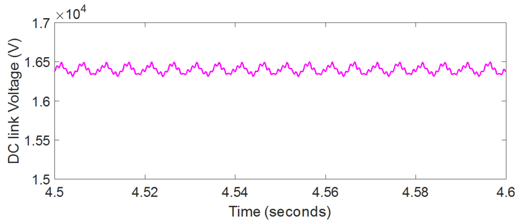

(f)

Figure 4.11: a) MMC UPS input voltage b) Load Voltage c) MMC UPS input current and d) Load current e) Average Cell Voltages f) DC link Voltage

Figure 4.11e shows the DC link voltage with an average voltage of 16400V that is stable and it is well distributed within the cells of the MMC that show voltage balancing as shown in Figure 4.11f.

5

Case Study

5.1 Problem Description

In low voltage power systems with power back up systems, there is a tendency to switch between different power sources and this results into de-energization and re-energization of transformers back and forth. With this background such networks are likely to suffer from consequences of inrush current. This case study in Figure 5.1 consists of an Emergency Power System (EPS) in a distribution network with Low voltage UPS installations to protect sensitive loads from power disturbances of short duration and also to provide backup power to the loads as the generators are started.

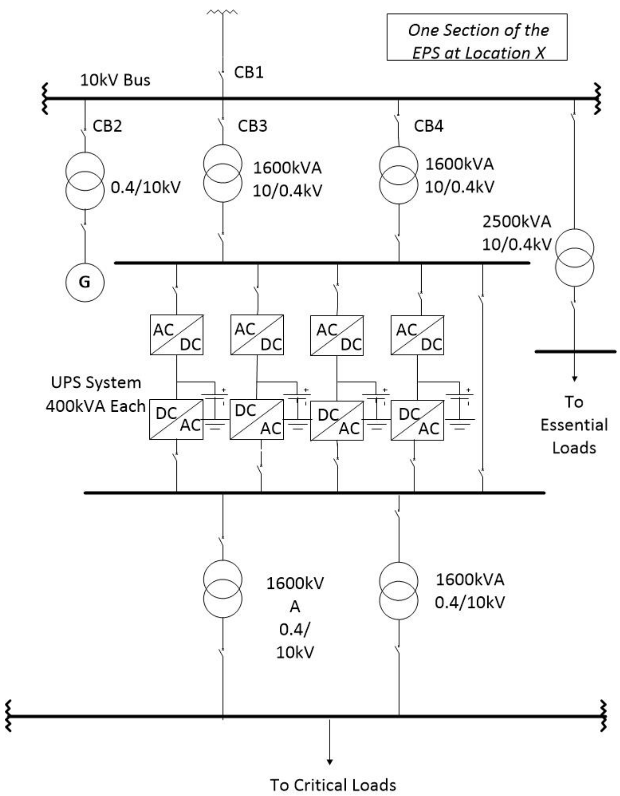

Figure 5.1: Emergency Power System in a distribution system

The Figure 5.1 is Part of a section of the network that is extracted to demonstrate the effects of transformer energizing in low voltage networks. This case study shows where the proposed MV MMC based UPS system can be utilized. In Figure 5.1 during normal operation, the sensitive load is fed through the UPS while the essential loads are fed directly from the mains and the emergency generator is off. In the event of an interruption, the generators are activated and they take around 30s to load and energize the 10kV bus during which time the sensitive load is continuously supplied by the UPS. At the instant of transferring the load to the generators, the up-stream transformers are energized and this leads to inrush currents due to transformer excitation.

5.2 Simulation of the Problem

The case study shown in the Figure 5.1 was implemented in Matlab/SIMULINK as shown in Figure 5.2. Since the main cause of inrush currents in electric distribution networks is saturation of the magnetic core of the transformer [28], the simulation was performed on unloaded transformers without the UPS loads connected. At 100ms, the circuit breaker was closed and line current measurements were done as well as voltage measurements on the 10kV bus. Two saturable step down transformers of 1.6MVA, 10/0.4kV were used in the model. Harmonics analysis was done using the powergui tool in Matlab/SIMULINK

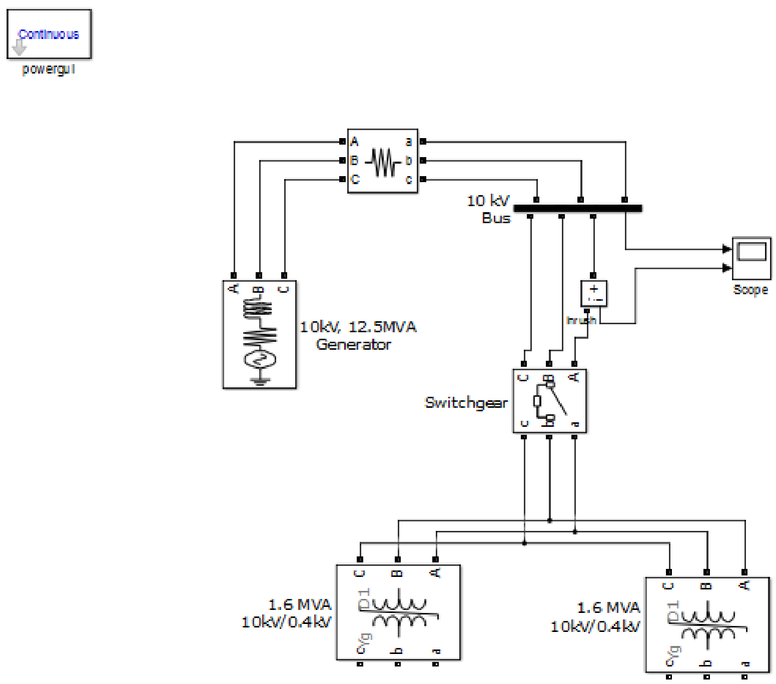

Figure 5.2: Simulation model for Inrush currents in the Network

Simulation results in the Figure 5.3a showed that there were inrush currents, the first peak of the inrush currents was 208A for the particular section of the network in the simulation and the duration of the inrush currents is over 1s. However, this may not be the case for a practical network since in the simulation the transformers that were used had a negligible winding resistance and that resulted into oscillations in the inrush currents. If measurements are done on a practical network, the duration of inrush currents may be in hundreds of milliseconds owing to the transformer winding resistance that damps the flux offset and the inrush currents decay to steady state.

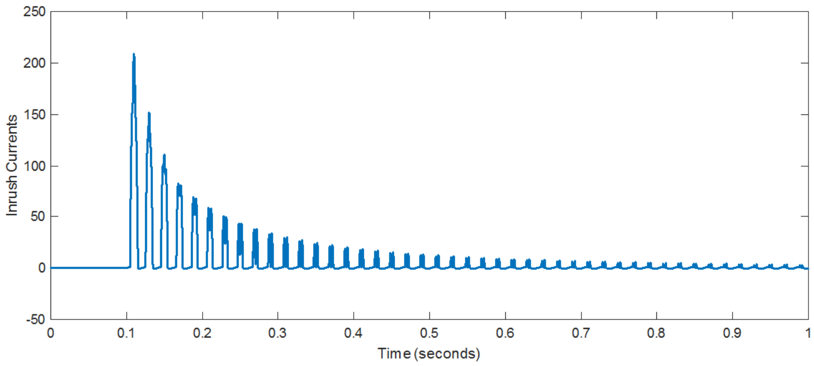

(a)

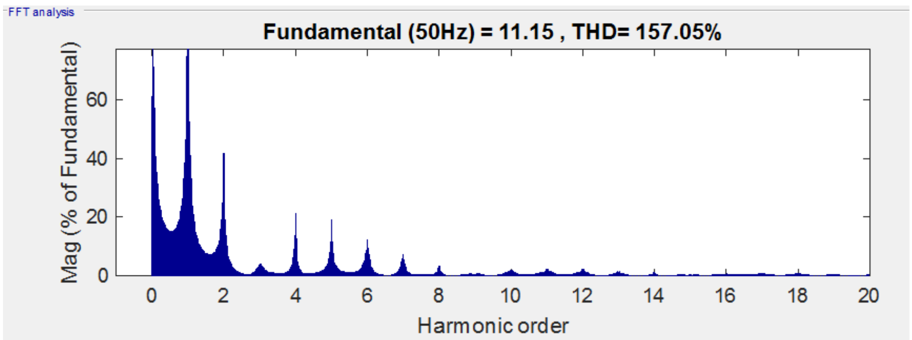

(b)

Figure 5.3: Voltage (a) Magnitude of inrush currents due to transformer energizing (b) Harmonic analysis of Inrush currents due to transformer energizing

Harmonic analysis of these inrush currents is shown in the Figure 5.3b and it shows that there are high second harmonics in the inrush currents. The inrush currents due to transformer energizing are usually observed in one set of windings and their corresponding current transformers and are likely to appear as a fault to the protective relays [29]. The consequence of these kind of negative sequence harmonics is that they may result into mis-operation of system protection and may cause unnecessary trips of the fuses and circuit breakers without any apparent reason [13]. The second harmonics need to be filtered out and this can be achieved by using transformer differential relay with harmonic filtering capabilities.

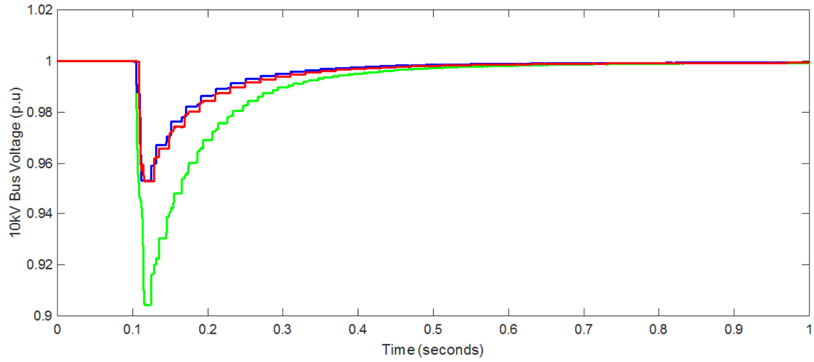

Figure 5.4: Voltage dip at the 10kV Bus due to Transformer energizing

Figure 5.4 shows the r.m.s voltages per phase in p.u at the 10kV bus due to inrush currents from transformer energizing. It was also observed from Figure 5.4 that the inrush currents led to a 0.9p.u unbalanced voltage dip on the 10kV bus. This resulted from the flow of the inrush currents through the series impedance of the between the power source and the transformer itself. Other essential loads farther downstream on this bus will suffer the effects of the dip.

5.3 Solution with M2C UPS system

Among the current industrial practices to mitigate inrush currents is to add external components to improve on the overload capability of the network. Over time these components age due to effects of temperature and require periodic maintenance. Addition of these components reduces the reliability of the network and makes it hard for the customer to comply with IEC standards on safety. An evaluation for the selection of the most suitable inrush current limiting devices are discussed in [30].

With the adoption of the medium voltage MMC UPS, it will enable medium voltage operation of the UPS system since the MMC UPS enables the series connection of cells to obtain higher operating voltages. Medium Voltage operation reduces the number of mains transformers upstream on the medium voltage network and/or number of isolation transformers. This solution can eliminate inrush currents. In addition to medium voltage operation of the UPS system, the MMC UPS system offers very high reliability compared to the Two-level converter based UPS system because a failed cell in the arm of the MMC can be bypassed and replaced while the UPS remains under operation. The MMC UPS system also requires smaller filters due to the more sinusoidal nature of the wave forms at the output of the MMC. Owing to the requirement of smaller filters and elimination of some transformers in the network, there is a significant reduction in the footprint area of the MMC UPS system.

6

Conclusion and Future work

6.1 Conclusion

The Medium Voltage MMC based UPS with half bridge modules is a promising candidate for the future UPS. It puts up better performance in-terms of power quality by having more sinusoidal converter output voltage wave forms. During the simulations it was observed that the MMC based UPS system because of this property required smaller output filters in relation to its power level compared to the Two-level converter based UPS system. The inductance of the MMC filter was 7.5mH comparable to 5mH for the Two-level converter based UPS system to achieve the similar UPS performance objectives in all the scenarios that were put under consideration. The Switching frequency of the MMC based UPS system was 1000Hz which was smaller than that used for the Two-level converter based UPS system at 2000Hz. Lower switching frequency meant lower converter losses hence a higher efficiency. The structure of MMCs was also described and it was observed that it offers more reliability than the Two-level converter based UPS system since a faulty cell in the arm can be by-passed or hot swapped while the UPS remains in operation. It was also shown that MMC based UPS systems at higher voltage levels which is possible through series connection of the cells in the structure of the MMC while still achieving cell voltage balancing of the cells.Operating a UPS at medium voltage means there will be a reduction in system losses. The MMC also allows the energy storage devices to be integrated into the cells of the converter while for the Two-level converter based UPS systems, the batteries can only be directly mounted onto the DC link. Integrating the batteries in the cells increases system redundancy of the MMC UPS systems. However, some design considerations of the transformerless MMC based UPS systems such as improvement of fault current handling capabilities and other grounding/safety requirements need to be addressed before it can fully be rolled out in the Medium Voltage power distribution network

6.2 Future Work

The thesis considered UPS systems with MMC that have half bridge modules. With full bridge modules there are enhanced capabilities of the MMC such as the addition of short circuit proofing where the full bridge are turned off with the help of appropriate gate signals and this ensures that current does not flow from the AC side to feed a DC fault on the DC link [31]. This will imply that an Isolation transformer would not be needed. It's therefore recommended that the UPS be re-modeled into a UPS with full-bridge MMC modules.

A study should be made to ascertain the optimal location and number of the isolation transformers that are required for various UPS applications with respect to grounding and safety requirements for both transformer based UPS systems as well as for the MMC based UPS.

It is suggested that a study be done to evaluate various existing solutions for static transfer switches for UPS applications in the industry.

The scope of the IEC standard, IEC 62040-3, for specifying UPS performance and test methods is limited to UPS installations up-to 1kV hence there are no existing standards for MV UPS installations despite their vast benefits. It is suggested that test scenarios and methods to specify performance for MV UPS systems should be done.

Bibliography

[1] S. Skok, S. Minea, and V. Niksa, "Electrical performance test procedure for uninterruptible power supplies," *IEEE*, no. 1, pp. 27–50, 2004.

[2] J. Gurrero, G. Luis De Vicu, and J. Uceda, "Uninterruptible power supply systems provide protection," *Industrial Electronics Magazine, IEEE*, vol. 1, pp. 28–38, 2007.

[3] D. Torstensson, "Swedish survey on cost of power outages," in *ERGEG Workshop on Continuity of Supply Regulation by Incentives - Willingness to Pay and Accept, Lisbon*, vol. 1. IEEE, September 2008.

[4] X. Liu, "Grounding system of an uniterruptible power system (ups)," in *Telecommunications Energy Conference, IEEE 30th International*, vol. 1. IEEE, 2008.

[5] J. Solanki, J. Bocker, F. Norbert, and P. Wallmeier, "A modular multilevel converter based high-power high-current power supply," *Industrial Technology (ICIT), 2013 IEEE International Conference*, pp. 444–450, 2013.

[6] A. SLega, S. Munk-Nielsen, F. Blaabjerg, and D. Casadei, "Multilevel converters for ups applications: comparison and implementation," *Power Electronics and Applications, 2007 European Conference*, pp. 1–9, 2007.

[7] P. Asimakopoulos, M. Bongiorno, and K. Papastergiou, "Design of a modular multilevel converter as an active front-end for a magnet supply application," *IEEE*, 2015.

[8] R. Thierry, B. Regine, N. Buchheit, and G. Frederic, "Power Quality Improvement - Case Study of the connection of Four 1.6 MVA Flywheel Dynamic UPS System to a Medium Voltage Distribution Network," *IEEE*, 2001.

[9] M. H. Bollen, *Understanding power quality problems.* IEEE press, 2000.

[10] Department of the US Army, *Uninterruptible Power Supply System Selection, Installation and Maintenance for Command, Control, Communications, Computer, Intelligence, Surveillance, and Reconnaissance (C4ISR) Facilities.*

IEEE, 2002.

[11] C. Loeffler and E. Spears, “UPS Basics,” *Eaton*, 2015.

[12] Emerson Network Power, “Comparing transformer-free to transformer-based ups designs,” *Liebert Corporation*, 2012.

[13] SQUARE D, “Power system harmonics, causes and effects of variable frequency drives relative to ieee 519-1992 standard,” *SQUARE D Product Data Bulletin, Raleigh, NC, USA*, 1994.

[14] J. Steele, “Transformerless UPS systems and the 9900,” *MITSUBISHI Electric*, 2010.

[15] M. Bongiorno, E. Behrouzian, and M. Beza, “Lecture notes: ENM075 Power Electronic Solutions for Power Systems.” Department of Energy and Environment, Chalmers University of Technology, Göteborg, Sweden, 2016.

[16] N. Mohan, T. M. Undeland, and W. P. Robbins, *Power Electronics Converters, Applications and Design.* John Wiley and Sons, Inc, 2003.

[17] J.-N. Fiorina, “Using of IGBT in UPS,” *MGE UPS Systems.*

[18] E. Wang and S. Huang, “A control strategy of three-phase voltage-sourced pwm rectifier.” Electrical Machines and Systems (ICEMS), 2011 International Conference, 2011.

[19] M. Beza, *Power System Stability Enhancement Using Shunt-connected Power Electronic Devices with Active Power Injection Capability (Phd Thesis).* Chalmers University of Technology, Göteborg, 2015.

[20] C. Chao, P. A. Grain, S. Finney, and B. Williams, “H-bridge modular multilevel converter: control strategy for improved dc fault ride through capability without converter blocking,” *IET Power Electronics*, 2015.

[21] C. Gomath, Navyanagath, S. Purnima, and S. Veerakumar, “Comparison of PWM Methods for Multilevel Inverter, ,” *International Journal of Advanced Research in Electrical, Electronics and Instrumentation Engineering*, no. 2, pp. 6106–6114, 2013.

[22] R. Ottersten, *On Control of Back-to-Back Converters and Sensorless Induction Machine Drives (Phd Thesis).* Chalmers University of Technology, Göteborg, 2003.

[23] W. Jun, B. Rolando, and D. Boroyevich, “A survey on the modular multilevel converters- modeling, modulation and controls,” *IEEE*, 2013.

[24] MATLAB®/Simulink®, 2016. [Online]. Available: www.mathworks.com

[25] PLECS®, "HVDC Transmission System with MMCs," Accessed on February 14, 2016. [Online]. Available: http://www.plexim.com/support/application-examples/938

[26] J. Svensson, *Grid-Connected Voltage Source Converter - Control Principles and Wind Energy Applications (Phd Thesis).* Chalmers University of Technology, Göteborg, 1998.

[27] M. Lindgren, *Modeling and Control of Voltage Source Converters Connected to the Grid (Phd Thesis).* Chalmers University of Technology, Göteborg, 1998.

[28] N. Chiesa, *Power Transformer Modeling for Inrush Current Calculation (PhD Thesis).* Norwegian University of Science and Technology, Trondheim, 2010.

[29] N. John, P, "A better understanding of harmonic distortion in the petrochemical industry," *IEEE*, 2002.

[30] K. Ruchi, Harchandaniand Rashmi, "Selection of effective mitigation method for inrush current in power transformer," *International Journal of Advanced Technology in Engineering and Science*, no. 1, pp. 359–366, 2014.

[31] O. Anaya-Lara, D. Campos-Gaona, E. Moreno-Goytia, and G. Adam, *Power Electronics Converters, Applications and Design.* John Wiley and Sons, Inc, 2014.

[32] M. Bongiorno, *On Control of Grid-connected Voltage Source Converters, Mitigation of Voltage Dips and Subsynchronous Resonances (Phd Thesis).* Chalmers University of Technology, Göteborg, 2007.

A

Appendices

A.1 Transformations from Three Phase to Rotating Reference Frames

The three phase system that consists of the following quantities, $v_a(t)$, $v_b(t)$ and $v_c(t)$ can be transformed into the rotating reference frame by first transforming it into the complex reference frame ($\alpha\beta$ -frame). The transformation in (A.1) below can be applied in this case [32],

$$\underline{v}(t) = v_\alpha + jv_\beta = K\left[v_a(t) + v_b(t)e^{j\frac{2}{3}} + v_c(t)e^{j\frac{4}{3}}\right] \tag{A.1}$$

where the K factor is $\frac{3}{2}$ or $\sqrt{\frac{3}{2}}$ to ensure voltage or power invariance respectively. For power-invariant transformation, (A.1) in matrix form is given as shown in (A.2)

$$\begin{bmatrix} v_\alpha(t) \\ v_\beta(t) \end{bmatrix} = M_{23} \begin{bmatrix} v_a(t) \\ v_b(t) \\ v_c(t) \end{bmatrix} \tag{A.2}$$

where,

$$M_{23} = \begin{bmatrix} \sqrt{\frac{3}{2}} & \frac{-1}{\sqrt{6}} & \frac{-1}{\sqrt{6}} \\ 0 & \frac{1}{\sqrt{2}} & \frac{-1}{\sqrt{2}} \end{bmatrix} \tag{A.3}$$

and,

$$\begin{bmatrix} v_a(t) \\ v_b(t) \\ v_c(t) \end{bmatrix} = M_{23}^{-1} \begin{bmatrix} v_\alpha(t) \\ v_\beta(t) \end{bmatrix} \tag{A.4}$$

If we consider the $\alpha\beta$-frame, and the vectors $\underline{v}(t)$ and $\underline{u}(t)$ rotate in the anti clockwise direction with angular frequency $\omega(t)$, thus they appear to be stationary in the dq-plane. Taking the vector $\underline{u}(t)$ on the d-axis in the dq-plane, then the vector $\underline{v}(t)$ will have two components in the dq-plane, one a projection on the direction of $\underline{u}(t)$ and the other in the orthogonal direction [32] as shown in the figure A.1

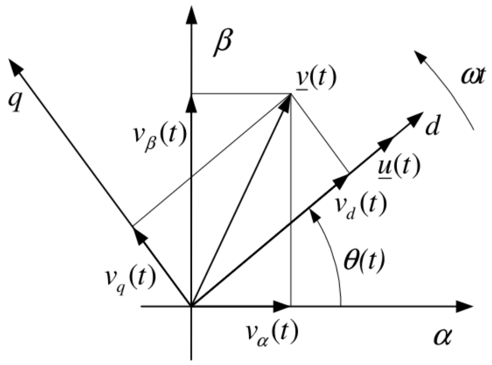

Figure A.1: Transformation to and fro $\alpha\beta$ and abc frames

The transformation from stationary - $\alpha\beta$ reference frame to the rotating reference frame - dq can be described by the (A.5) below.

$$\underline{v}^{dq}(t) = \underline{v}^{\alpha\beta}(t)e^{-j\theta(t)} \tag{A.5}$$

where,

$$\theta(t) = \theta_0 + \int_0^t \omega(\tau)d\tau \tag{A.6}$$

Conversely,

$$\underline{v}^{\alpha\beta}(t) = \underline{v}^{dq}(t)e^{j\theta(t)} \tag{A.7}$$

In the matrix form, (A.8) and (A.9) below can be used for transformations between the $\alpha\beta$ - and the dq - coordinate system

$$\begin{bmatrix} v_d(t) \\ v_q(t) \end{bmatrix} = \begin{bmatrix} \cos\theta & -\sin\theta \\ \sin\theta & \cos\theta \end{bmatrix} \begin{bmatrix} v_\alpha(t) \\ v_\beta(t) \end{bmatrix} \tag{A.8}$$

and

$$\begin{bmatrix} v_\alpha(t) \\ v_\beta(t) \end{bmatrix} = \begin{bmatrix} \cos\theta & \sin\theta \\ -\sin\theta & \cos\theta \end{bmatrix} \begin{bmatrix} v_d(t) \\ v_q(t) \end{bmatrix} \tag{A.9}$$

A.2 MMC UPS UPS System

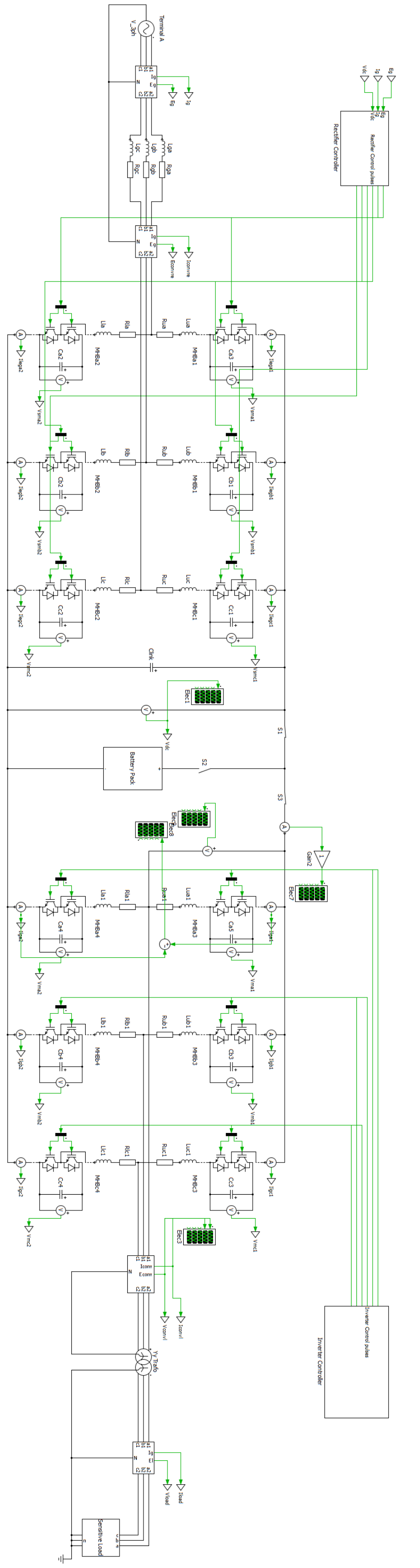

Figure A.2: PLECS Simulation model for MMC based UPS System

A.3 MMC Rectifier Controller

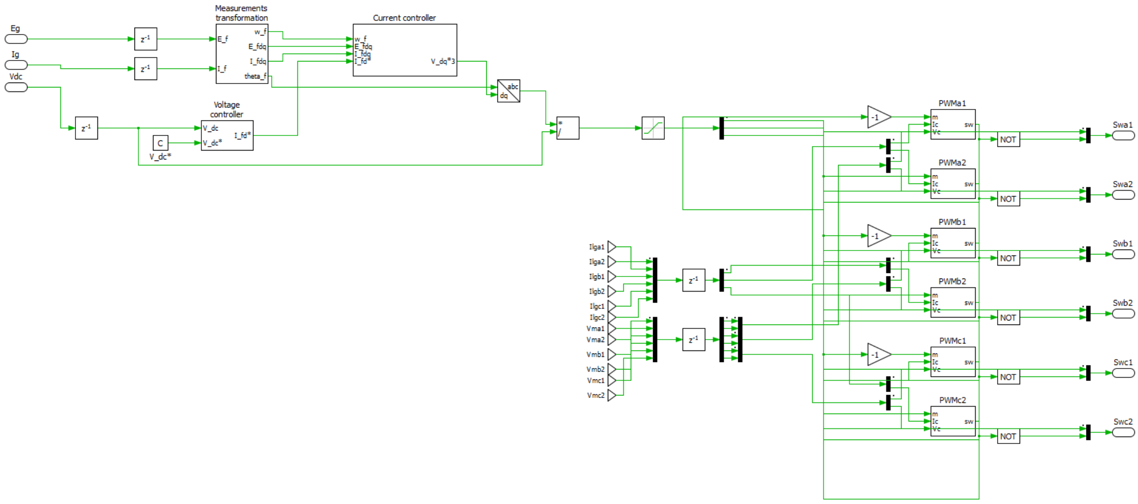

Figure A.3: Control for the MMC rectifier

A.4 MMC Load side Controller

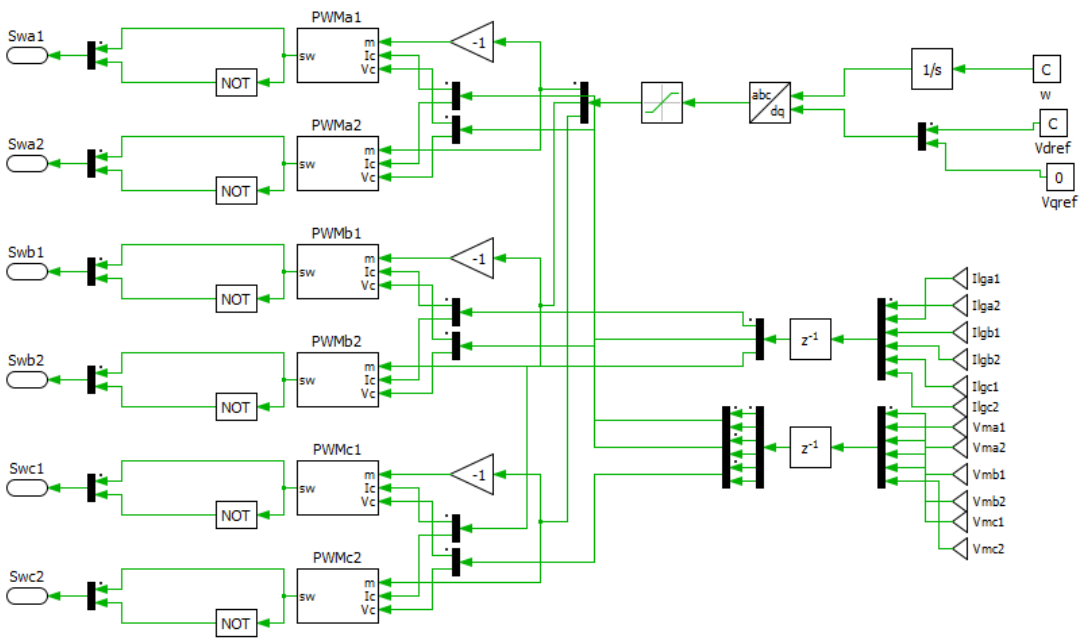

Figure A.4: Control for MMC Load side converter

A.5 Two Level UPS System

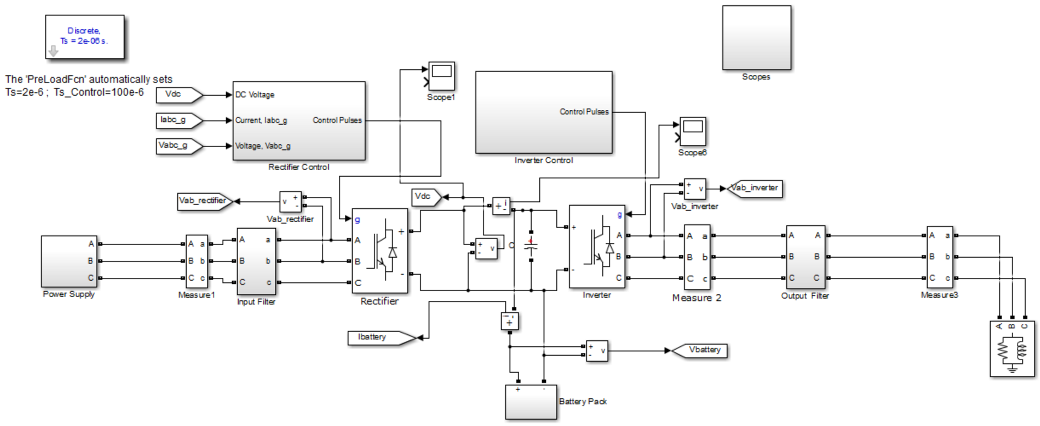

Figure A.5: SIMULINK Simulation model for Two level VSC based UPS System

A.6 Controller for the two level VSC

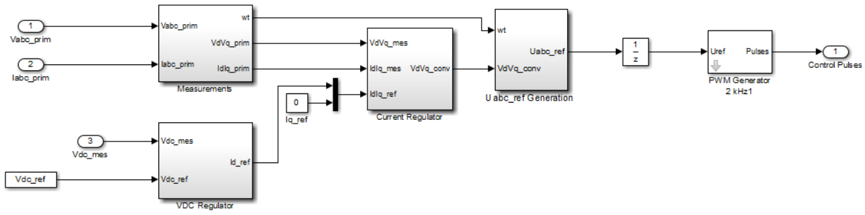

Figure A.6: Control for the two level VSC

A.7 Controller for the two level load connected converter

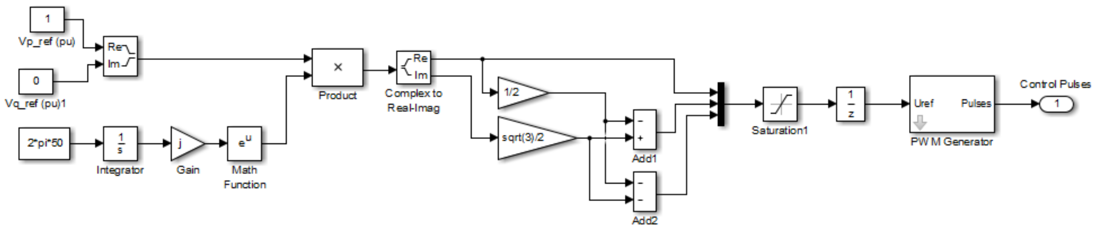

Figure A.7: Control for the two level load connected converter

A.8 Lead Acid Battery

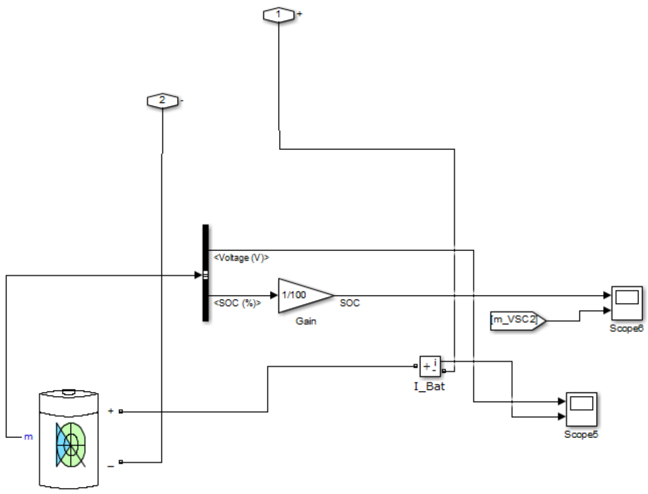

Figure A.8: SIMULINK Lead Acid Battery